The long noncoding RNA HIF1a-AS1 regulates endothelial cell function and is increased in patients with aortic valve disease and coronary artery disease

Inaugural-Dissertation

zur Erlangung des Doktorgrades

der Hohen Medizinischen Fakultät

der Rheinischen Friedrich-Wilhelms-Universität

Bonn

Ling Zhou

aus Chongqing/China

2023

Angefertigt mit der Genehmigung
der Medizinischen Fakultät der Universität Bonn

1. Gutachter: PD Dr. med. Felix Jansen
2. Gutachterin: Prof. Dr. Kerstin Wilhelm-Jüngling

Tag der Mündlichen Prüfung: 30. Nov. 2023

Aus der Medizinischen Klinik II - Innere Medizin (Kardiologie, Pneumologie)
Direktor: Prof. Dr. med. Georg Nickenig

Table of Contents

List of abbreviations

ACTD	Actinomycin D
aSMA	a-smooth muscle actin
AVS	aortic valve stenosis
BrdU	bromodeoxyuridine
BMP	bone morphogenetic protein
CAD	coronary artery disease
CAVD	calcific aortic valve disease
CHX	cycloheximide
CVD	cardiovascular disease
CVDs	cardiovascular diseases
DAPI	4′,6-diamidino 2phenylindole
ECs	endothelial cells
EndMT	endothelial to mesenchymal transition
EVs	extracellular vesicles
HCAECs	human coronary artery endothelial cells
HIF1a	Hypoxia-Inducible Factor 1 Alpha
HIF1a-AS1	Hypoxia-Inducible Factor 1 Alpha Antisense 1
HIF1a-AS2	Hypoxia-Inducible Factor 1 Alpha Antisense 2
HUVECs	human umbilical vein endothelial cells
IL1β	interleukin-1β

LDH	lactate dehydrogenas
LDL	low-density lipoprotein
LncRNAs	long noncoding RNAs
ncRNAs	non-coding RNA
NF-KB	nuclear factor kappa-B
oxLDL	oxidized low-density lipoprotein
ox-PLs	oxidized phospholipids
siRNA	small interfering RNA
TGFβ	transforming growth factor beta
THBS1	Thrombospondin-1
TNF-α	tumor necrosis factor alpha
VSMCs	vascular smooth muscle cells
VE-cadherin	vascular endothelial cadherin

1. Introduction

1.1 Cardiovascular diseases

Cardiovascular disease (CVD) is a group of disorders that affect the heart and blood vessels. It remains a leading cause of morbidity and mortality worldwide, accounting for an estimated 17.9 million deaths in 2019 (GBD 2017 Causes of Death Collaborators, 2018). The pathogenesis of CVD is complex, involving multiple genetic and environmental factors. The development of atherosclerosis, which is characterized by the buildup of plaque within the arterial walls, is a key mechanism underlying many forms of CVD. Among the various subtypes of CVD, coronary artery disease (CAD) and aortic valve stenosis (AVS) are two of the most common conditions that require clinical attention.

CAD is a condition characterized by the narrowing or blockage of the coronary arteries due to the buildup of plaque, which can ultimately lead to myocardial infarction and/or sudden cardiac death (Libby, 2021). It is responsible for approximately 1 in 7 deaths in the United States (Benjamin, et al., 2019). CAD is a complex disease involving multiple mechanisms, including oxidative stress, inflammation, lipid metabolism dysfunction, and endothelial dysfunction, all of which contribute to the development of atherosclerotic lesions in the coronary arteries (Hansson and , et al., 2011, Libby, 2013). Endothelial dysfunction is an early event in the pathogenesis of CAD. It is characterized by impaired production and bioavailability of nitric oxide, which contributes to vasoconstriction, platelet activation, and leukocyte adhesion (Cyr, et al., 2020). Endothelial dysfunction also leads to increased permeability of the arterial wall, allowing for the infiltration of low-density lipoprotein (LDL) cholesterol and immune cells into the subendothelial space (Widmer, et al., 2014). The accumulation of LDL cholesterol in the arterial wall triggers an inflammatory response, characterized by the recruitment of monocytes and T lymphocytes. Activated inflammatory cells release cytokines, chemokines, and growth factors that promote further recruitment of immune cells and smooth muscle cells, leading to the formation of atherosclerotic plaques (Tabas, 2010). Chronic inflammation plays a critical role in the progression of atherosclerotic lesions. Inflammatory mediators such as interleukin-6, C-reactive protein, and tumor necrosis factor alpha (TNF-α) have been shown to promote plaque instability and rupture, leading to acute coronary syndromes (Libby, et al., 2011).

Similar to CAD, AVS operates through a shared mechanism of action, where reduced blood flow prompts the heart to engage in augmented efforts to deliver adequate blood supply throughout the body. The presence of AVS serves as an effective surrogate marker for cardiovascular events that are causally linked to CAD. It is worth noting that both these pathological conditions are comprehensively encompassed by atherosclerotic disease, rendering them amenable to similar clinical interventions and preventive measures.

AVS is a type of cardiovascular disease caused by calcific aortic valve disease (CAVD), which is characterized by the narrowing of the aortic valve and reduced blood flow from the heart to the rest of the body. The pathogenesis of CAVD is a complex process involving multiple factors, including endothelial dysfunction, lipid deposition, oxidative stress, inflammation, and genetic predisposition (Rajamannan, 2011). Valvular endothelial cells (VECs) play an important role in maintaining valvular homeostasis by producing protective factors such as nitric oxide and prostacyclin (Manduteanu, et al., 1988, Siney, et al., 1993). However, in response to various stresses, including shear stress and inflammation, these cells can become activated, leading to upregulation of pro-inflammatory cytokines, chemokines, and adhesion molecules that promote leukocyte recruitment and subsequent valvular inflammation (Butcher, et al., 2011). Proinflammatory cytokines such as interleukin-1β (IL1β), TNF-α, and osteopontin have been shown to promote calcification and fibrosis of the valve leaflets by promoting osteogenic differentiation and calcification of valvular interstitial cells (VICs), which express markers of both smooth muscle cells and fibroblasts (Mohler, et al., 2001, Aikawa, et al., 2007). Furthermore, mutations in genes encoding proteins involved in the regulation of valvular homeostasis, such as NOTCH1 and LRP5, have also been associated with the development of AVS (Nigam, et al., 2009, Rajamannan, 2011).

The development of CAVD can be seen as two distinct phases (Figure 1). The first phase is characterized by lipid deposition, injury, and inflammation. Oxidized low-density lipoprotein (ox-LDL) accumulates in the aortic valve leaflets, triggering an inflammatory response that leads to the recruitment of immune cells such as macrophages and T cells into the valve tissue (Rajamannan, 2011). These immune cells release proinflammatory cytokines, which promote calcification and fibrosis of the valve leaflets (Mohler, et al., 2001). Mechanical stress, such as hypertension or shear stress, can also trigger injury and inflammation in the valve tissue (Aikawa, et al., 2007). This phase sets the stage for

the subsequent propagation of CAVD. The second phase involves osteogenic differentiation and calcification of valve tissue. Valve interstitial cells differentiate into osteoblast-like cells, which express bone morphogenetic proteins (BMPs) and other signaling molecules that promote extracellular matrix mineralization (Rajamannan, et al., 2003, Aikawa, et al., 2006, Nigam, et al., 2009). Calcium deposits accumulate in the valve leaflets, leading to stiffening and reduced mobility of the valve cusps. The increased expression of receptor activator of nuclear factor kappa-B (NF-KB) ligand and decreased expression of osteoprotegerin in VICs have been implicated in the development of calcific aortic valve disease (Willems, et al., 1994). As the disease progresses, the valve becomes increasingly calcified and stenotic, leading to impaired cardiac function and ultimately heart failure.

Endothelial-to-mesenchymal transition (EndMT) is a cellular process that has been associated with the development of atherosclerosis and AVS, and it is controlled by numerous interacting pathways. Notch, transforming growth factor (TGFβ), and Wingless/integrated-1 signaling pathway β-catenin-dependent pathway (Wnt/β-catenin) are some of the key pathways involved in EndMT (Combs and Yutzey, 2009). For instance, TGFβ is known to be a powerful inducer of EndMT (Mahler, et al., 2013), and activates the Wnt/β-catenin signaling pathway by promoting the translocation of β-catenin to the nucleus, where it acts as a transcription factor (Liebner, et al., 2004). On the contrary, Notch pathway activation leads to an elevation in TGFβ levels and triggers the activation of transcription factors, including Zinc finger protein and SNAI1/2. Subsequently, this results in a reduction of Vascular Endothelial Cadherin (VE-cadherin), compromising the endothelial barrier function (Timmerman, et al., 2004). EndMT is characterized by an increase in cell invasion and motility, a decrease in endothelial markers such as vascular endothelial cadherin, and overexpression of myofibroblast markers such as a-smooth muscle actin (aSMA) (Paranya, et al., 2001). Moreover, EndMT is involved in atherosclerosis by inducing a number of phenotypes ranging from endothelial cell dysfunction to plaque formation (Evrard, et al., 2016). EndMT-derived fibroblast-like cells show higher amounts of matrix metalloproteinase than normal fibroblasts, which is associated with unstable atherosclerotic plaques (Furman, et al., 2004, Schneider, et al., 2008). Risk factors associated with atherosclerosis and AVS, such as persistent inflammation, fluid shear stress, oxLDL, and smoking, can contribute to EndMT.

Additionally, TGFβ signaling, oxidative stress, and hypoxia enhance the change of endothelial cells (ECs) to mesenchymal cells and are all defining characteristics of atherosclerosis and AVS (Chen, et al., 2020). Valve interstitial cells (VICs) can also undergo phenotypic changes to become osteoblast and myofibroblast-like VICs, which are responsible for active calcium deposition in AVS (Wirrig and Yutzey, 2014).

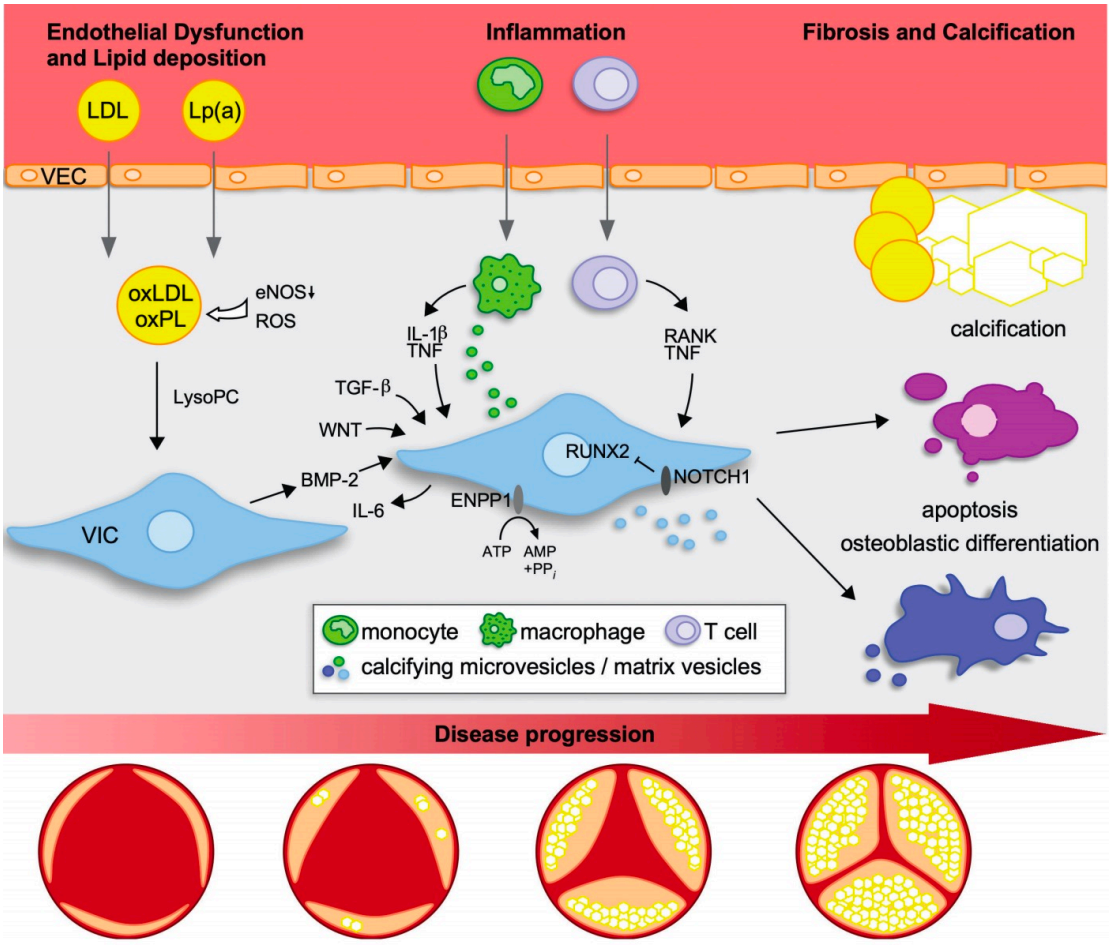

Fig. 1: Schematic diagram of the phases of calcific aortic valve disease (CAVD). CAVD can be divided into several stages: endothelial dysfunction and lipid accumulation, inflammation, fibrosis, and calcification. Valvular endothelial cells (VECs) can become dysfunctional due to mechanical or shear stress, resulting in the infiltration of low-density lipoprotein (LDL) and lipoprotein[a] (Lp(a)). Reactive oxygen species can be produced as a result of eNOS pathway dysregulation, leading to further oxidation of the infiltrated lipids into oxidized LDL (ox-LDL) and ox-PLs (oxidized phospholipids). Immune cells can enter the tissue and secrete TNF (tumor necrosis factor), Interleukin-1β (IL1β), Interleukin-6, and receptor activator of nuclear factor kappa B (RANKL), promoting osteogenic differentiation of VICs. The release of matrix vesicles/calcifying microvesicles can further accelerate calcification (Modified from Goody PR, et al., 2020).

1.2 Long noncoding RNAs

More than 98 % of the genome does not encode proteins which are called non-coding RNA (ncRNAs). Evidence shows that ncRNAs are one of the major regulatory networks of gene expression at the epigenetic, transcriptional, and even post-transcriptional levels (Kaikkonen, et al., 2011, Patil, et al., 2014, Palazzo, et al., 2015). NcRNAs are critical regulators of cardiovascular function and thus candidates for reliable biomarkers that can be used in clinical practice. Furthermore, ncRNAs now fundamentally act as novel therapeutic options for CVD (Poller, et al., 2018). Long non-coding RNAs (lncRNAs) are a class of RNA molecules that are longer than 200 nucleotides in length and do not code for proteins. In the recent years, lncRNAs have been found to play important roles in various biological processes, including CVD.

Several lncRNAs have been implicated in the development of CVD, such as ANRIL and MALAT1 (Holdt, et al., 2016). For example, ANRIL has been shown to regulate the expression of genes involved in vascular smooth muscle cell proliferation and migration, which are crucial processes in the pathogenesis of atherosclerosis (Holdt, et al., 2016). MALAT1 has been linked to the regulation of endothelial cell function and the development of pulmonary arterial hypertension (Zhao, et al., 2016). Additionally, lncRNAs have been proposed as potential biomarkers for the diagnosis and prognosis of CVD. For instance, a study showed that low expression of the lncRNA MIAT was associated with an increased risk of adverse cardiovascular events in patients with coronary artery disease (Ishii, et al., 2006). Besides, lncRNAs may govern gene expression in the nucleus or regulate other cytoplasmic processes, such as RNA stability, to carry out their intended purpose. (Kumarswamy, et al., 2014, Uchida, et al., 2015). Our previous study revealed that extracellular vesicles (EVs) are one of the most important carriers of circulating ncRNAs, protecting them from circulating RNases and improving their plasma stability (Liu, et al., 2019, Zietzer, et al., 2020, Hosen, et al., 2021, Hosen, et al., 2022). EVs have been reported to play important roles in intercellular communication and the transfer of biological molecules, including lncRNAs (Gan, et al., 2020).

EVs are small membrane-bound particles that are released by various cell types, including immune cells, cancer cells, and stem cells. EVs can be divided into two subtypes based

on their size: large EVs, which are typically between 100 and 1000 nm in diameter and are formed by outward budding of the plasma membrane, and small EVs, which are typically between 30 and 100 nm in diameter and are formed by the inward budding of multivesicular bodies before being released into the extracellular space (Théry, et al., 2018). Moreover, EV-mediated transfer of lncRNAs between cells has emerged as an important mechanism for intercellular communication and gene regulation. In particular, the transfer of lncRNAs by EVs could modulate the function of target ECs and further influence disease progression. For example, EV-associated lncRNAs have been implicated in the regulation of inflammation, angiogenesis, and apoptosis in ECs, all of which play important roles in CVD pathogenesis (Chen, et al., 2017).

Recent studies have identified three lncRNAs that are transcribed from the same genomic locus as HIF1a. These lncRNAs are known as HIF1a antisense RNA 1 (HIF1a-AS1), HIF1a antisense RNA 2 (HIF1a-AS2), and HIF1a antisense RNA 3 (HIF1a-AS3). Interestingly, HIF1a can induce the expression of HIF1a-AS1 and HIF1a-AS2 under hypoxic conditions, HIF1a-AS1 has been identified as a negative regulator of HIF1a, while the expression of HIF1a-AS3 is negatively regulated by HIF1a (Chen, et al., 2017, Li, et al., 2017, Rodríguez-Lorenzo, et al., 2020). Moreover, recent studies have shown that HIF1a is significantly upregulated in AVS and contribute to the pathogenesis of AVS (Salim, et al., 2022). These lncRNAs have been found to play important roles in the atherosclerosis-related pathological conditions. HIF1a-AS1, for instance, has been found to be involved in inhibiting vascular smooth muscle cells (VSMCs) proliferation by upregulating TGFβ1 (Xu, et al., 2019). HIF1a-AS2 has been identified as a "sponge" for miR-153-3p, which can reduce the post-transcriptional silencing of HIF1a by miR-153-3p, thus regulating endothelial cell function (Li, et al., 2017). Similarly, our recent study revealed that a number of lncRNA including HIF1a-AS1 are significantly upregulated in CAD (Hosen, et al., 2021). CAD and AVS are both associated with the development of atherosclerosis and share similar risk factors such as hypertension and hyperlipidemia. As a result, our research aims to investigate the role of the lncRNA HIF1a-AS1 in AVS and its potential association with HIF1a-AS2 due to their shared mechanisms.

These lncRNAs have the potential to serve as biomarkers and therapeutic targets for AVS. Further research is needed to fully understand the molecular mechanisms underlying the functions of these lncRNAs in AVS and to evaluate their clinical applications.

1.3 Objectives

Therefore, the specific aims of this study can be outlined as follows:

1. To explore the biological function of HIF1a-AS1/ HIF1a-AS2 in endothelial cells.
2. To investigate the underlying molecular mechanism of HIF1a-AS1-induced endothelial phenotype change.
3. To investigate the involvement of HIF1a-AS1 in EndMT of valvular endothelial cells and its influence in pathophysiology of AVS.

2. Materials and Methods

2.1 Materials

Tab. 1: Chemicals and Reagents

Materials	Company	Catalog number
Actinomycin D	Sigma-Aldrich	A4262-2MG
Bromodeoxyuridine (BrdU)	BD Biosciences	550891
Cycloheximide (CHX)	Cell Signaling Technology	2112S
DAPI	Vector laboratories	H-1200
Growth Factor Reduced Matrigel	Thermo Fisher Scientific	A1413202
HIF1a-AS1 siRNA	Thermo Fisher Scientific	4427037
HIF1a-AS2 siRNA	Thermo Fisher Scientific	4390771
Interleukin-1β (IL1β)	R&D Systems	201-LB-010
Lipofectamine RNAimax	Thermo Fisher Scientific	13778150
Negative Control siRNA	Thermo Fisher Scientific	AM4611
oxLDL	Thermo Fisher Scientific	L34357
Polyacrylamide Gels	BioRad	4561084
Polyvinylidene Fluoride Membrane	Thermo Fisher Scientific	88585
Protease Inhibitor Cocktail	Roche	11873580001
RIPA buffer	Sigma-Aldrich	R0278
RT2 Profiler PCR array RT2 Human Angiogenesis	QIAGEN	PAHS-024Z

TGFβ	R&D Systems	240-B-010
THBS1 (thrombospondin 1) siRNA	Thermo Fisher Scientific	4392420
TNF-α	R&D Systems	300-01A-250UG
TRIzol	Thermo Fisher Scientific	15596018

Tab. 2: Commercial Kits

Materials	Company	Catalog number
ECL™ Prime Western Blotting Detection Kit	Sigma-Aldrich	RPN2232
High Capacity cDNA Reverse Transcription Kit	Thermo Fisher Scientific	4368813
LDH Cytotoxicity assay kit	Thermo Fisher Scientific	88953
MTT Cell Growth Assay Kit	Sigma-Aldrich	CT02
Qubit™ Protein Assay Kit	Thermo Fisher Scientific	Q33211
RNeasy Mini Kit	QIAGEN	74104
RT2 First Strand Kit	QIAGEN	330401

Tab. 3: Cells

Materials	Company	Catalog number
Human Coronary Artery Endothelial Cells (HCAECs)	Promocell	C-12221

Human Umbilical Vein Endothelial Cells (HUVECs)	Promocell	C-12200
Human Aortic Valve Endothelial Cells (hAoVECs)	Lonza	00225975

Tab. 4: Medium

Materials	Company	Catalog number
Endothelial Cell Growth Medium	Promocell	C-22010
Endothelial Cell Growth Medium MV	Promocell	C-22020
Growth Medium MV Supplement Mix	Promocell	C-39225
Growth Medium Supplement Mix	Promocell	C-39215

Tab. 5: Primers (TaqMan)

Materials	Company	Catalog number
aSMA/ACTA2 (Hs00426835_g1)	Thermo Fisher Scientific	4351370
HIF1a (Hs00153153_m1)	Thermo Fisher Scientific	4453320
HIF1a-AS1 (Hs04407794_m1)	Thermo Fisher Scientific	4331182
HIF1a-AS2 (Hs03454328_s1)	Thermo Fisher Scientific	4426961

NOS3 (Hs01574665_m1)	Thermo Fisher Scientific	4331182
TAGLN/SM22a (Ss03373216_g1)	Thermo Fisher Scientific	4351372
THBS1 (Hs00962908_m1)	Thermo Fisher Scientific	4331182
von Willebrand factor (Hs01109446_m1)	Thermo Fisher Scientific	4331182

Tab. 6: Antibodies

Materials	Company	Catalog number
Anti-beta-Actin antibody	Sigma-Aldrich	A1978
Anti-BrdU antibody	Abcam	ab6326
Anti-CD31 antibody	Abcam	ab28364
Anti-histone H3 antibody	Abcam	ab1791
Anti-Mouse IgG	Sigma-Aldrich	A9044-2ML
Anti-Rabbit IgG	Sigma-Aldrich	A9169-2ML
Anti-SM22 alpha antibody	Abcam	ab14106
Anti-Thrombospondin 1 antibody	Abcam	ab85762
Anti-Vimentin antibody	Abcam	ab8978
Donkey Anti-Rabbit-Cy3 IgG antibody	Jackson Immuno Research	712-165-153
Goat Anti-Rabbit-Cy3 IgG antibody	Dianova	111-165-144

Tab. 7: Equipment

Materials	Company	Catalog number
Applied Biosystems 7500HT Real-Time PCR	Thermo Fisher Scientific	-
Applied Biosystems 7900HT Real-Time PCR	Thermo Fisher Scientific	-
Falcon Permeable Support for 12-well Plate with 1.0 µm	Corning	353103
Falcon 12-well TC-treated Polystyrene Permeable	Corning	353503
Lab-Tek chambered 4-well chambered Cover glass	Thermo Fisher Scientific	155383PK
Nanodrop spectrophotometer	Thermo Fisher Scientific	-
Qubit-4 fluorometer	Thermo Fisher Scientific	-

2.2 Methods

2.2.1 RNA isolation and qRT-PCR

Total RNA was extracted and isolated using the TRIzol method according to the manufacturer's instructions. RNA was diluted in UltraPure DNase/RNase-Free Distilled Water (Invitrogen). The concentration and purity of the total RNA (absorbance at 260/280 nm [A260/A280] and A260/A230) was quantified using a Nanodrop spectrophotometer (Nanodrop Technologies). Total RNA was then reverse transcribed using a High Capacity cDNA Reverse Transcription Kit (Thermo Fisher Scientific, #43-688-13) according to the manufacturer's protocol. mRNAs were detected using TaqMan gene expression assays (Thermo Fisher Scientific) on a 7500 HT real-time PCR instrument (Applied Biosystems).

For all mRNAs, a CT value above 45 was defined as undetectable. Values are expressed as $2^{-[CT\ (miR)-\ CT\ (control)]}\ log_{10}$, and samples were run in triplicate.

2.2.2 Cell culture and generation

ECs (PromoCell) were cultured in cell growth basal media with growth media supplement mix (PromoCell, # C-22010, C-22020) under standard conditions (37 °C, 5 % CO_2). HUVECs and HCAECs from passages 6-8, VECs from passages were used when they were 70-80 % confluent.

2.2.3 Centrifugation of extracellular vesicles

After treatment based on different experimental designs, confluent cells were starved by incubation in basal medium (without growth media supplements) for 24 hours, and the supernatant was collected for centrifugation after starvation. To isolate large EVs from the culture medium or plasma supernatant, samples were first centrifuged at 2000 × g, 4 °C for 15 minutes to remove cell debris. The supernatant was collected and centrifuged again at 20,000 × g, 4 °C for 40 minutes to pellet the EVs. The EV pellet was resuspended in sterile, ice-cold PBS and then centrifuged again (20,000 × g, 4 °C, 40 min) to purify the EVs. The pure EV pellet was resuspended in sterile 1 × PBS and used fresh.

2.2.4 Stimulation of EC by using atherosclerotic stimuli in vitro

Confluent ECs were treated with PBS (control), 10 ng/mL, or 20 ng/mL oxLDL (Thermo Fisher Scientific, #L34357) for 24 hours. Similarly, ECs were treated for 24 hours with different TNF-α (R&D Systems, #300-01A-250UG) concentrations (10 ng/mL, 20 ng/mL). Total RNA was then isolated from oxLDL- or TNF-α-treated ECs using a TRIzol (Invitrogen) extraction method according to the manufacturer's instructions.

2.2.5 Transfection of EC

Transient small interfering RNA (siRNA) transfection (20 nM final concentration) of semiconfluent ECs (50 % - 60 % confluent) was performed. For siRNA HIF1a-AS1

experiments, ECs were transfected with HIF1a-AS1 siRNA (Thermo Fisher Scientific, #4427037) or negative control siRNA (Thermo Fisher Scientific, #AM4611) using Lipofectamine RNAimax (Thermo Fisher Scientific, #13778150) for 48 hours, according to the manufacturer's protocol. For siRNA THBS1 or HIF1a-AS2 experiments, ECs were transfected with THBS1 siRNA (Thermo Fisher Scientific, #4392420) or HIF1a-AS2 siRNA (Thermo Fisher Scientific, #4390771) or control siRNA (Thermo Fisher Scientific, #AM4611) using Lipofectamine RNAimax for 48 hours, according to the manufacturer's protocol.

2.2.6 Protein isolation and immunoblotting

Immunoblotting of ECs was homogenized in RIPA buffer (Sigma-Aldrich, # R0278) with 1:25 Protease Inhibitor Cocktail (Roche, #11873580001) on ice. Lysates were sonicated for 10 minutes and protein concentration was measured with a Qubit-4 fluorometer (Thermo Fisher Scientific) using a Qubit™ Protein Assay Kit (Thermo Fisher Scientific, # Q33211) according to the manufacturer's instructions. An equal amount of protein (30-50 ug) for the cells was applied to pre-made 4 % - 15 % polyacrylamide gels (BioRad, #4561084). The gel was then transferred to a polyvinylidene fluoride membrane (Thermo Fisher Scientific, #88585), followed by blocking in 5 % bovine serum albumin in Tris-buffered saline containing 0.1 % Tween 20 for 1 hour. Blots were incubated with the appropriate primary antibodies: Anti-Thrombospondin 1 antibody (Abcam, #ab85762); Anti-CD31 antibody (Abcam, #ab28364); Anti-Vimentin antibody (Abcam, #ab8978); Anti-SM22 alpha antibody (Abcam, #ab14106), and detection was performed with the corresponding secondary antibody: Anti-Rabbit IgG (Sigma-Aldrich, #A9169-2ML) or Anti-Mouse IgG (Sigma-Aldrich, #A9044-2ML). Membranes were imaged with chemiluminescence via an ECL™ Prime Western Blotting Detection Kit (SIGMA-Aldrich; #RPN2232). Analysis of the grayscale images of the Western blot bands was performed using Image J. Anti-beta-actin antibody (Sigma-Aldrich, #A1978-100UL) or anti-histone H3 antibody (Abcam, #ab1791) was used as a loading control.

2.2.7 mRNA stability

ECs were plated in a 6-well plate and incubated for 48 hours under optimal cell growth conditions (5 % CO_2 and 37 °C in an incubator). Cells were then induced with 5 mg/mL actinomycin D (Sigma-Aldrich, #A4262-2MG), which was added to the culture medium for 24 hours. Cells were incubated with Cycloheximide (CHX) (Cell Signaling Technology, #2112S). For CHX, 500 mg of CHX powder was dissolved in 5 mL of sterile DMSO and homogenized to make a 10 mg/mL stock solution. A similar number of cells were treated with CHX at a final concentration of 20 ug/mL for 24 hours. RNA from untreated cells was also collected as a control. Finally, samples were lysed with TRIzol and RNA was isolated for qRT-PCR analysis.

2.2.8 MTT assay

ECs were transferred to a 96-well plate containing 2000 cells/well in 100 µL medium at 37 °C and 5 % CO_2 overnight. 0.01 mL AB solution from an MTT Cell Growth Assay Kit (Sigma-Aldrich, #CT02) was added to each well and incubated at 37 °C for 4 hours. Wells with medium as control. 0.1 ml isopropanol containing 0.04 N HCl was added to each well and mixed thoroughly. Absorbance was measured using an ELISA plate reader (TECAN, Infinite M200 Microplate reader) at a test wavelength of 570 nm and a reference wavelength of 630 nm.

2.2.9 Cytotoxicity assay

Total lactate dehydrogenase (LDH) activity in cell lysates was examined using the LDH cytotoxicity assay kit (Thermo Fisher, #88953) according to the manufacturer's instructions. Cells were seeded in a 96-well plate with 2000 cells per well in 100 µL medium at 37 °C and 5 % CO_2 overnight. Wells with medium as control. Add 10 µL of sterile water and 10 µL of lysis buffer to the control group and incubate the plate for 45 minutes at 37 °C and 5 % CO_2 in the incubator. Transfer 50 µL of each sample medium to a new 96-well plate and mix with 50 µL of the reaction mixture. After 30 minutes of light protected incubation at room temperature, the reactions were stopped by adding a "stop" solution. Absorbance at 490 nm and 680 nm was measured using an ELISA plate reader to determine LDH activity.

2.2.10 Co-incubation of ECs with transfected ECs and EVs

ECs were cultured in serum-free medium for 24 hours, and EVs were isolated after 24 hours according to the protocol described above. Co-incubation of endothelial EVs and recipient ECs for 24 hours. Then, ECs were washed three times with PBS. Total RNA was isolated from all EC samples for qRT-PCR analysis. We performed a transwell experiment with HIF1a-AS1-silenced donor cells and compared them with control ECs. Donor cells were transfected with HIF1a-AS1 siRNA and a scramble control (siSCR) for 24 hours and then seeded into a 1.0 µm insert (Corning, #353103). Recipient cells were seeded into 12-well plates (Corning, #353503) and co-incubated with the donor cells and recipient cells for 24 hours by placing the insert on the plates. Total RNA was isolated from the recipient samples for qRT-PCR analysis ECs.

2.2.11 THBS1 immunostaining

Immunocytochemistry of ECs was performed with Anti-Thrombospondin 1 antibody (Abcam, #ab85762). 5×10^4 ECs per well were grown in a Cover glass 4-well chambered slide (Lab-Tek chambered, #155383PK). 24 hours after seeding, cells were rinsed with PBS and fixed with 4 % paraformaldehyde in PBS for 10 minutes at RT. The fixed cells were washed with PBS and incubated with 0.25 % Triton X-100 in PBS for 10 min at room temperature to permeabilize the cell membranes. After three washing steps with PBS, cells were incubated with the blocking solution (0.25 % Triton X-100; 1 % BSA in PBS) for 1 hour at room temperature. Subsequently, the cells were incubated with Anti-Thrombospondin 1 antibody (Abcam, #ab85762) 1:500 in the blocking solution overnight at 4 °C. After washing extensively with PBS three times, cells were incubated with Goat Anti-Rabbit-Cy3 IgG antibody (Dianova, #111-165-144) for 60 minutes at RT protected from light. After washing with PBS, 4′,6-diamidino-2-phenylindole (DAPI) staining (Vector laboratories, #H-1200) was performed. Images were acquired using a Zeiss Axio Observer inverted microscope and analyzed using ZEN 2.3 pro software.

2.2.12 RT2 Profiler angiogenesis PCR array gene expression

Total RNA was isolated from ECs using an RNeasy Mini Kit (QIAGEN, #74104) according to the manufacturer's instructions. Subsequently, 1 mg of total RNA was reverse

transcribed using an RT2 First Strand Kit (QIAGEN, #330401) according to the manufacturer's protocol. RT2 Profiler PCR array RT²Human Angiogenesis (QIAGEN, #PAHS-024Z) was performed to measure the expression of 84 key genes involved in modulating the biological processes of angiogenesis. PCR was performed on an Applied Biosystems 7500 HT real-time PCR instrument. The comparative Cycle of Threshold (Ct) method was performed to calculate the relative expression of the transcripts.

2.2.13 Proliferation assay by fluorescence microscopy

3×10^4 cells/well ECs were seeded overnight in 24-well plates. Cells were then pulsed with Bromodeoxyuridine (BrdU) (10 µM, BD Biosciences, #550891) for 6 hours. Cells were fixed and denatured. BrdU incorporation was detected with Anti-BrdU antibody (Abcam, #ab6326) and a secondary antibody Donkey Anti-Rabbit-Cy3 IgG antibody (Jackson ImmunoResearch, #712-165-153). Cell nuclei were stained with DAPI (Vector laboratories, #H-1200). A Zeiss Axiovert 200M microscope and ZEN 2.3 pro software were used for imaging.

2.2.14 Tube formation assay

After overnight thawing at 4 °C, 100 mL of Growth Factor Reduced Matrigel (Thermo Fisher Scientific; #A1413202) was added to each well of the cold 24-well plates using cold pipette tips, and the plates were then stored for 2 hours at room temperature. 3×10^4 ECs were added to each of the Matrigel-coated wells and incubated for 24 hours under standard cell culture conditions (37 °C, 5 % CO_2). Tube formation was quantified by measuring the number of nodules and total tube length. Digital images of sections of microtiter wells were acquired using a Zeiss Axiovert 200 M microscope and ZEN 2.3 Pro software. Data were analyzed using Image J image analysis software (NIH, USA).

2.2.15 EndMT induction

ECs were plated at a density of 9×10^4 in 6-well culture plates and then transfected with HIF1a-AS1 siRNA or control siRNA for 48 hours as mentioned above. Subsequently, these ECs were treated with TNF-α (0.3 ul/mL, Prepotech, #300-01A) or (5 ul/mL, R&D

Systems, #240-B-010) and IL1β (2 ul/mL, R&D Systems, #201-LB-010) for 5 consecutive days under standard cell culture conditions (37 °C, 5 % CO_2) and refreshed every 48 hours. For qRT-PCR analysis, total RNA was isolated from the obtained EC samples.

2.2.16 Statistical analysis

Continuous variables with normal distribution were expressed as mean ± SD, and their normal distribution was tested using the Kolmogorov-Smirnov test. Categorical variables were presented as frequencies and percentages. To compare continuous variables between two groups, either Student's t test or Mann-Whitney U test was employed. For comparisons involving more than two groups, separate measures test ANOVA with Bonferroni's correction for multiple comparisons was used. A p-value < 0.05 was considered statistically significant, and all tests were two-sided. GraphPad Prism 8 was utilized for statistical analysis.

3. Results

3.1 HIF1a-AS1 is upregulated upon stimulation of atherosclerotic stimuli in vitro

HIF1a-AS1 has been reported to be significantly increased in patients with AVS and CAD, both of which are known to be associated with the development of atherosclerosis. Therefore, we hypothesize that HIF1a-AS1 may play a role in atherosclerosis development, and its expression is altered under atherosclerotic conditions. To investigate whether pro-atherosclerotic conditions could regulate cellular HIF1a-AS1 expression in vitro, we quantified HIF1a-AS1 expression in ECs after stimulation with increasing levels of oxLDL or TNF-α. Interestingly, oxLDL or TNF-α induced an increased HIF1a-AS1 expression in ECs (Figure 2A-B). In summary, this finding suggests that atherosclerotic stimuli (oxLDL and TNF-α) could upregulate the expression of HIF1a-AS1, which may play a role in atherosclerosis development.

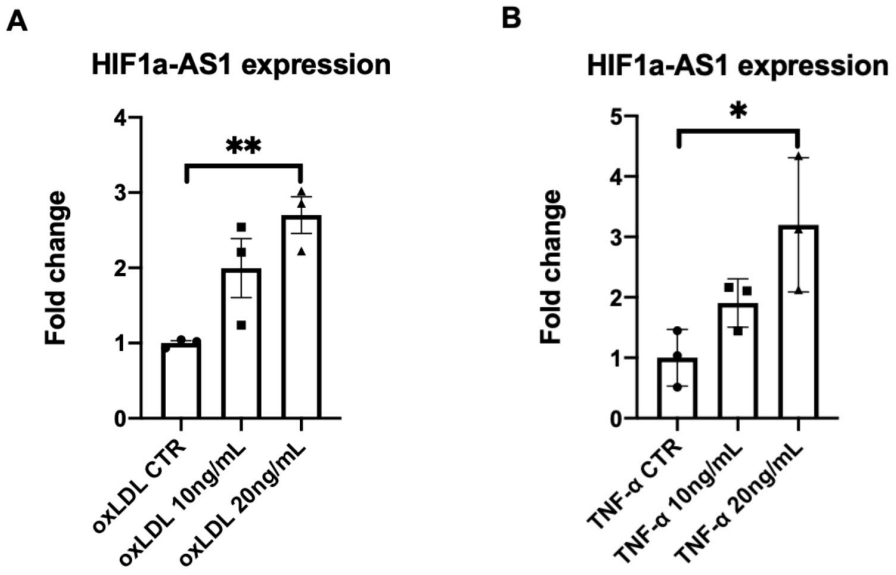

Fig. 2: Atherosclerotic stimuli increase HIF1a-AS1 expression in endothelial cells (ECs). (A and B) HIF1a-AS1 was analyzed in ECs after stimulation with different concentrations of oxidized low-density lipoprotein (oxLDL) or tumor necrosis factor alpha (TNF-α) for 24 hours by qRT-PCR (*$p < 0.05$, **$p < 0.01$, $n = 3$, by 1-way ANOVA with Bonferroni correction for multiple comparisons test). The cycle threshold

(CT) values were normalized to the expression of GAPDH and presented as fold changes. Data represent mean ± SD.

3.2 HIF1a-AS1 and HIF1a-AS2 regulate ECs function

Given the pivotal role of ECs in the development and progression of atherosclerosis and AVS, along with previous reports on the regulatory functions of HIF1a-AS1 and HIF1a-AS2 in modulating EC activity, our study aims to investigate the roles of HIF1a-AS1 and HIF1a-AS2 within the context of endothelial cells. Building upon prior research insights, our primary objective is to elucidate the impact of HIF1a-AS1 and HIF1a-AS2 on EC proliferation and the formation of tubular structures, while also assessing the protective role of HIF1a-AS1 in endothelial cells.

To achieve this, we initiated our study with the transfection of ECs using siRNA targeting HIF1a-AS1 and HIF1a-AS2, and subsequently validated the efficacy of HIF1a-AS1 and HIF1a-AS2 downregulation via qRT-PCR in ECs, as depicted in Figure 3A.

Furthermore, we assume that knocking down HIF1a-AS1 could have a protective effect on ECs. We employed the MTT and LDH assays, which serve as indirect indicators of cell viability and cytotoxicity, respectively. The MTT assay measures mitochondrial activity, often correlated with cell viability, while the LDH assay assesses LDH release, a marker of cell membrane damage and cell death. The results of the MTT and LDH assays provide support for our conclusions, as the downregulation of HIF1a-AS1 corresponded with the highest cell viability and the lowest cytotoxicity levels (Figure 3B-C). These assays suggest that HIF1a-AS1 knockdown may exert a protective effect on ECs by promoting cell survival and reducing cell death.

Subsequently, the downregulation of HIF1a-AS1 led to an increase in EC proliferation (Figure 3D-E) and enhanced tube formation capabilities (Figure 3F-H). Similarly, the knockdown of HIF1a-AS2 promoted in vitro EC proliferation (Figure 3D-E), whereas no significant differences were observed between the scramble control and the HIF1a-AS2 downregulation group in the tube formation assay (Figure 3F-H).

Our investigation has revealed that HIF1a-AS1 and HIF1a-AS2 likely play significant roles in the regulation of EC proliferation and the angiogenesis process. Specifically, our findings indicate that HIF1a-AS1 functions as an anti-angiogenic and anti-proliferative transcript or lncRNA in ECs, while HIF1a-AS2 functions as an inhibitor of EC proliferation.

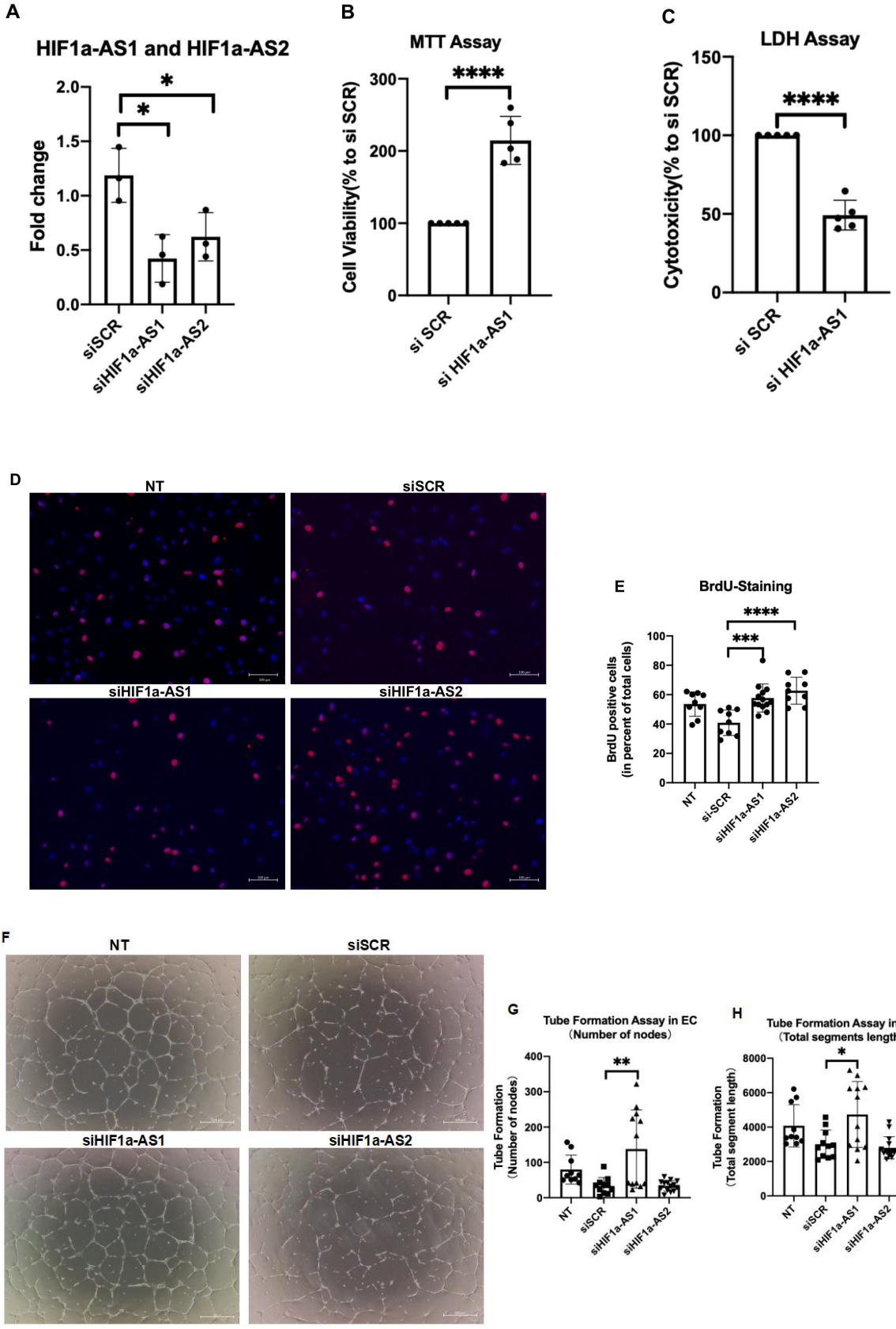
A
HIF1a-AS1 and HIF1a-AS2
Fold change
2.0
1.5
1.0
0.5
0.0
*
*
siSCR
siHIF1a-AS1
siHIF1a-AS2
B
MTT Assay
Cell Viability(% to si SCR)
300
200
100
0
****
si SCR
si HIF1a-AS1
C
LDH Assay
Cytotoxicity(% to si SCR)
150
100
50
0
****
si SCR
si HIF1a-AS1
D
NT
siSCR
siHIF1a-AS1
siHIF1a-AS2
E
BrdU-Staining
BrdU positive cells
(in percent of total cells)
100
80
60
40
20
0
****
***
NT
si-SCR
siHIF1a-AS1
siHIF1a-AS2
F
NT
siSCR
siHIF1a-AS1
siHIF1a-AS2
G
Tube Formation Assay in EC
(Number of nodes)
Tube Formation
(Number of nodes)
400
300
200
100
0
**
NT
siSCR
siHIF1a-AS1
siHIF1a-AS2
H
Tube Formation Assay in EC
(Total segments length)
Tube Formation
(Total segment length)
8000
6000
4000
2000
0
*
NT
siSCR
siHIF1a-AS1
siHIF1a-AS2

Fig. 3: HIF1a-AS1 and HIF1a-AS2 regulates the function of target ECs. (A) ECs were transfected with siRNA against HIF1a-AS1 and HIF1a-AS2, the efficiency of HIF1a-AS1 HIF1a-AS2 downregulation following siRNA transfection was confirmed using qRT-PCR in ECs. (*p < 0.05, n = 3, by Student's t test). (B and C) Cell death was measured using a LDH cytotoxicity assay (C), and cell viability of ECs was measured using an MTT assay (B) (****p < 0.0001, n = 5, by 1-way ANOVA with Bonferroni multiple comparisons test). (D and E) Bromodeoxyuridine (BrdU) incorporation was determined by immunofluorescence (red). Nuclei were stained with 4′,6-diamidino-2-phenylindole (DAPI, blue). The percentage of BrdU-positive cells was compared with the total number of cells (***p < 0.001, ****p < 0.0001, n > 6, by 1-way ANOVA with Bonferroni multiple comparisons test). Scale bars, 100 μm; ×100 magnification. In the BrdU assay, both siHIF1a-AS1 and siHIF1a-AS2 demonstrated a significantly higher number of BrdU-positive cells in comparison to NT and siSCR. (F and G and H) Tube formation assays of ECs. Capillary tubes were imaged with an immunofluorescence microscope. Total segment length and node number were measured and quantified using Image J image analysis software (*p < 0.05, **p < 0.01, n > 6, by 1-way ANOVA with Bonferroni multiple comparisons test). Scale bar, 500 μm; ×100 magnification. In the tube formation assay, siHIF1a-AS1 exhibited higher values for both node number and total segment length than NT and siSCR, whereas siHIF1a-AS2 displayed less distinct differences compared to NT and siSCR.

3.3 EV can transfer HIF1a-AS1 via large EVs

Although previous studies have demonstrated that EVs can deliver lncRNAs in various diseases, it remains unclear whether EV-mediated transfer of HIF1a-AS1 is possible. To investigate this, we conducted the co-cultured and transwell experiments to investigate the potential EV-mediated transfer of HIF1a-AS1.

Initially, we co-cultured EVs with ECs and observed that HIF1a-AS1 expression was down-regulated in ECs that were exposed to EVs generated from HIF1a-AS1-silenced donor cells transfected with HIF1a-AS1 siRNA (Figure 4A). The EVs were isolated from starved transfected ECs that were collected through a series of centrifugation steps as described previously. These findings provide evidence supporting the possibility of HIF1a-AS1 transfer from EVs to ECs.

Furthermore, to further confirm whether HIF1a-AS1 transfer mediated by EVs exists in vitro, we performed a transwell experiment with HIF1a-AS1-silenced donor cells and compared them with control ECs. We found that the expression of HIF1a-AS1 was reduced in recipient ECs that were co-cultured with HIF1a-AS1-silenced donor cells in the transwell assay (Figure 4B). In summary, our results suggest that EVs have the potential to transfer HIF1a-AS1 from donor cells to recipient ECs.

However, the expression of HIF1a-AS1 is slightly decreased in the siSCR group compared to the NT group in both experiments, indicating that factors such as cell culture conditions and transfection efficiency may have some influence on the results. Therefore, it is not possible to rule out the impact of these factors on the experimental results. Further evidence is needed to support the conclusion that there may be HIF1a-AS1 transfer from donor cells to recipient cells through EVs.

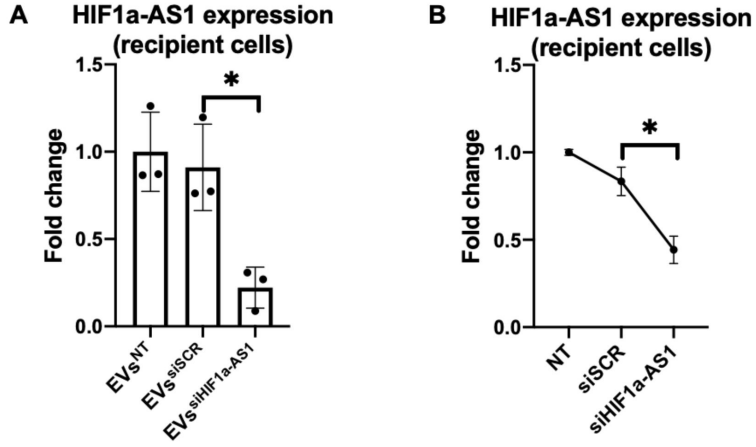

Fig. 4: Intercellular transfer of HIF1a-AS1 via large EVs in ECs. (A) HIF1a-AS1 expression was assessed in ECs that were treated with large endothelial vesicles (EVs) siHIF1a-AS1 or EVs scramble control (siSCR) or without any treatment (NT) using qRT-PCR. CT values were normalized to GAPDH and were expressed as fold change (*$p < 0.05$, $n = 3$, by Student's t test). (B) Transwell experiments with normal, siSCR, siHIF1a-AS1 in donor cells and recipient cells. Donor cells were transfected with HIF1a-AS1 small interfering RNA (siRNA) and siSCR for 24 hours. HIF1a-AS1 expression was quantified in recipient ECs after transwell with donor cells for 24 hours. GAPDH was used as a control (*$p < 0.05$, by Student's t test).

3.4 HIF1a-AS1 controls the angiogenic gene network and regulates THBS1 transcription and translation in ECs

The mechanism by which HIF1a-AS1 regulate EC proliferation and angiogenesis remains unclear. To explore the underlying mechanism of HIF1a-AS1 in regulating angiogenic functions in recipient ECs, RT2 profiler PCR array analysis was performed to measure differential expression of 84 key genes involved in modulating the biological processes of angiogenesis. The analysis of the array results revealed that the expression of THBS1 (thrombospondin 1), NRP1 (Neuropilin 1), AKT1 (AKT serine/threonine kinase 1), TIMP2 (TIMP metallopeptidase inhibitor 2), TIE1 (Tyrosine kinase with immunoglobulin-like and EGF-like domains 1) was significantly downregulated in target ECs when HIF1a-AS1 was

knocked down. Specifically, the fold change for THBS1 was 0.41, NRP1 was 0.35, AKT1 was 0.20, TIMP2 was 0.18 and TIE1 was 0.17 (Figure 5A).

To confirm these results, we performed a comprehensive set of experiments, including single qRT-PCR, immunoblotting, and Western blot experiments. In the single real-time PCR experiments, our results showed that among the target genes examined, only THBS1 was dysregulated in target ECs, and its expression increased upon HIF1a-AS1 knockdown (Figure 5B).

However, our investigation delved deeper into the protein-level changes. Through Western blot and immunoblotting analyses, we observed a contrary trend. The level of THBS1 protein determined by Western blot and immunoblotting decreased compared to control cells (Figure 5C-E). These results, while presenting a complex interplay between gene expression and protein levels, highlight the intricate regulatory mechanisms at play and emphasize the need for further exploration to fully comprehend the functional implications of HIF1a-AS1 in the context of THBS1 regulation in ECs.

Besides this, we also analyzed the upregulated gene expression upon HIF1a-AS1 knockdown, these genes including pro-angiogenic factor VEGFA (Vascular endothelia growth factor a), F3 (Coagulation factor III), as well as other cellular factors CCL2 (Chemokine (C-C motif) ligand 2), CXCL10 (C-X-C motif chemokine 10) and CXCL8 (C-X-C motif chemokine 8), were significantly upregulated (Figure 5A). Given that CCL2, CXCL10 and CXCL8 are commonly known cytokines associated with inflammation and endothelial dysfunction, it is likely that their upregulation upon knockdown of HIF1a-AS1 is due to the activation of inflammatory pathways. Single PCR and Western blot analyses were performed to confirm the upregulation of these genes, but no significant changes in their expression were observed upon knockdown of HIF1a-AS1.

Our study demonstrated that HIF1a-AS1 acts as an anti-angiogenic and anti-proliferative lncRNA in ECs, contrasting with the function of HIF1a-AS2, which acts as a gene promoting reduced proliferation in ECs. Moreover, We also found that EVs have the potential to transfer HIF1a-AS1 from donor cells to recipient ECs, indicating a possible mechanism for intercellular communication. Furthermore, our data suggested that HIF1a-AS1 may control the angiogenic gene network and regulate THBS1 transcription and translation in ECs, providing insights into the underlying mechanisms of angiogenesis regulation.

Previous studies have indicated that HIF1a-AS1 may have a more significant impact on endothelial cell function and angiogenesis compared to HIF1a-AS2 and HIF1a-AS3. Furthermore, it has been demonstrated that HIF1a-AS1 exerts a significant influence on the expression of THBS1, emphasizing its central role in the angiogenic process. Consequently, our subsequent experiments concentrated exclusively on deciphering the multifaceted effects of HIF1a-AS1 and its downstream targets.

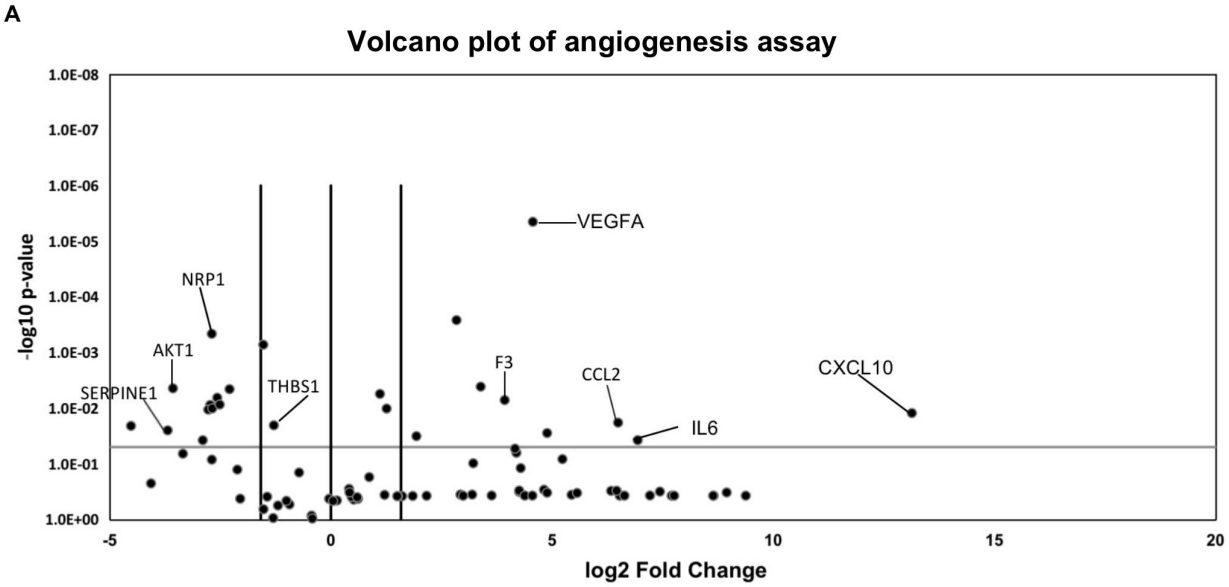

Top5 dysregulated gene in target ECs					
Downregulated	Fold Change	p value	Upregulated .	Fold Change	p value
THBS1	0.41	0.020289	VEGFA	23.66	0.000004
NRP1	0.35	0.000721	F3	29.59	0.027954
AKT1	0.20	0.004547	CXCL8	89.95	0.018169
TIMP2	0.18	0.008593	CCL2	122.30	0.037547
TIE1	0.17	0.006475	CXCL10	8972.74	0.012223

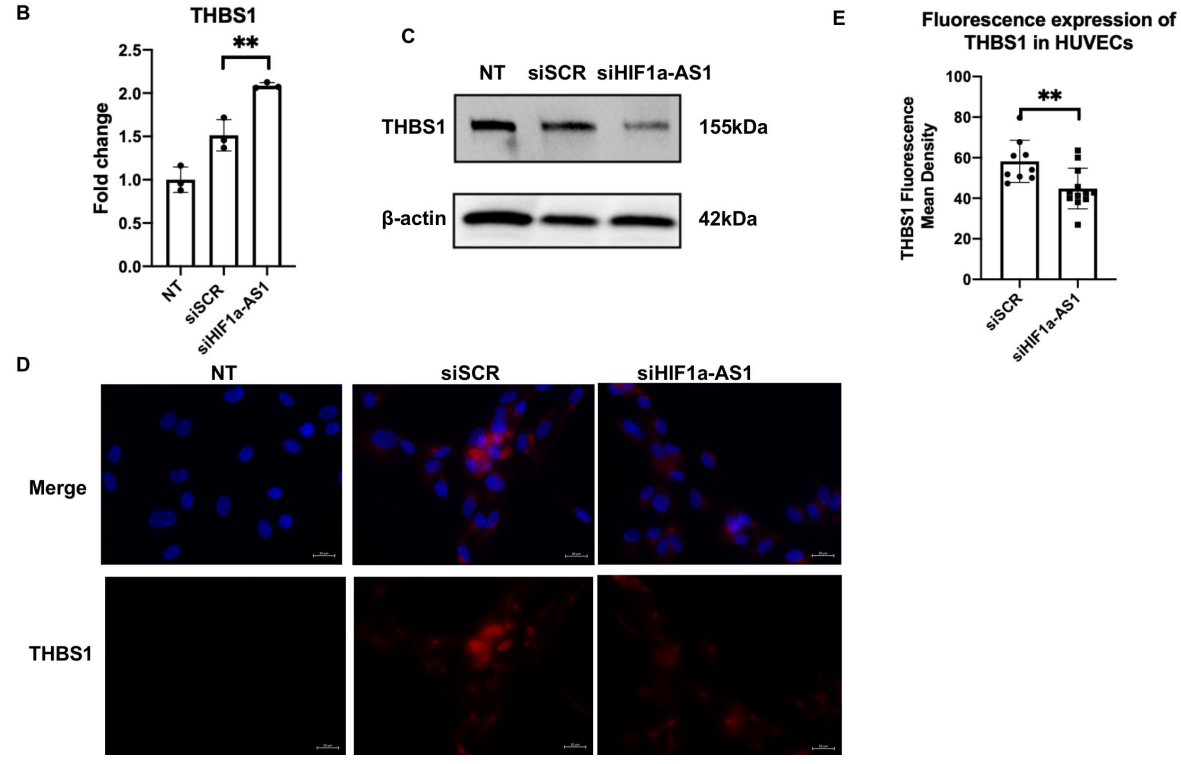

Fig. 5: HIF1a-AS1 RNA regulates the level of THBS1 (thrombospondin 1) in ECs. RT^2 Profiler PCR array analyses (angiogenesis) were performed on ECs transfected with HIF1a-AS1 siRNA and control (n = 3). Ribosomal protein lateral stalk subunit P0

(RPLP0; as PCR array control) was used as an endogenous control in the PCR array. (A) A volcano plot shows the differentially regulated genes between HIF1a-AS1 knockdown and control ECs by PCR array, as well as the top 5 dysregulated genes in ECs. (B) Individual validation of THBS1 RNA expression was conducted in ECs transfected with HIF1a-AS1 siRNA and siSCR using qRT-PCR. (**$p < 0.01$, $n = 3$, by 1-way ANOVA with Bonferroni multiple comparisons test). (C) THBS1 protein levels were assessed by Western blot in ECs that were transfected with HIF1a-AS1 siRNA and siSCR. β-Actin was used as the loading control. (D and E) Immunocytochemical staining of THBS1 (red), nuclear staining with DAPI (blue). Relative quantification of THBS1 fluorescence expression was measured by qRT-PCR (**$p < 0.01$, $n > 6$, by 1-way ANOVA with Bonferroni multiple comparisons test). Scale bars, 20 μm; × 400 magnification. As illustrated in Fig. 5 D and E, the fluorescence expression of THBS1 (red) was notably lower in comparison to siSCR and NT.

3.5 THBS1 regulates the EC function

The previous experimental results suggest that HIF1a-AS1 is a gene that inhibits angiogenesis. Inhibition of HIF1a-AS1 at the RNA level leads to increased expression of THBS1 mRNA. However, at the protein level, the expression of THBS1 is decreased. The relationship between HIF1a-AS1 and THBS1 in angiogenesis is complex and not fully understood. We hypothesize that HIF1a-AS1 may regulate endothelial cell function by controlling THBS1 expression, and therefore, we need to further investigate the role of THBS1 in endothelial cells. To investigate the role of THBS1 in EC angiogenesis and proliferation, siRNA against THBS1 was transfected into ECs, and efficient downregulation was confirmed by real-time PCR (Figure 6A). The downregulation of THBS1 led to a significant increase in both EC tube formation and proliferation, highlighting the importance of THBS1 as a negative regulator of EC angiogenesis and proliferation (Figure 6B-F). Taken together, these results suggest that HIF1a-AS1 and THBS1 play important roles in the regulation of angiogenesis, with HIF1a-AS1 inhibiting angiogenesis and THBS1 acting as a negative regulator of angiogenesis. HIF1a-AS1 may inhibit angiogenesis by downregulating THBS1 expression at the protein level and potentially through other mechanisms that are yet to be elucidated.

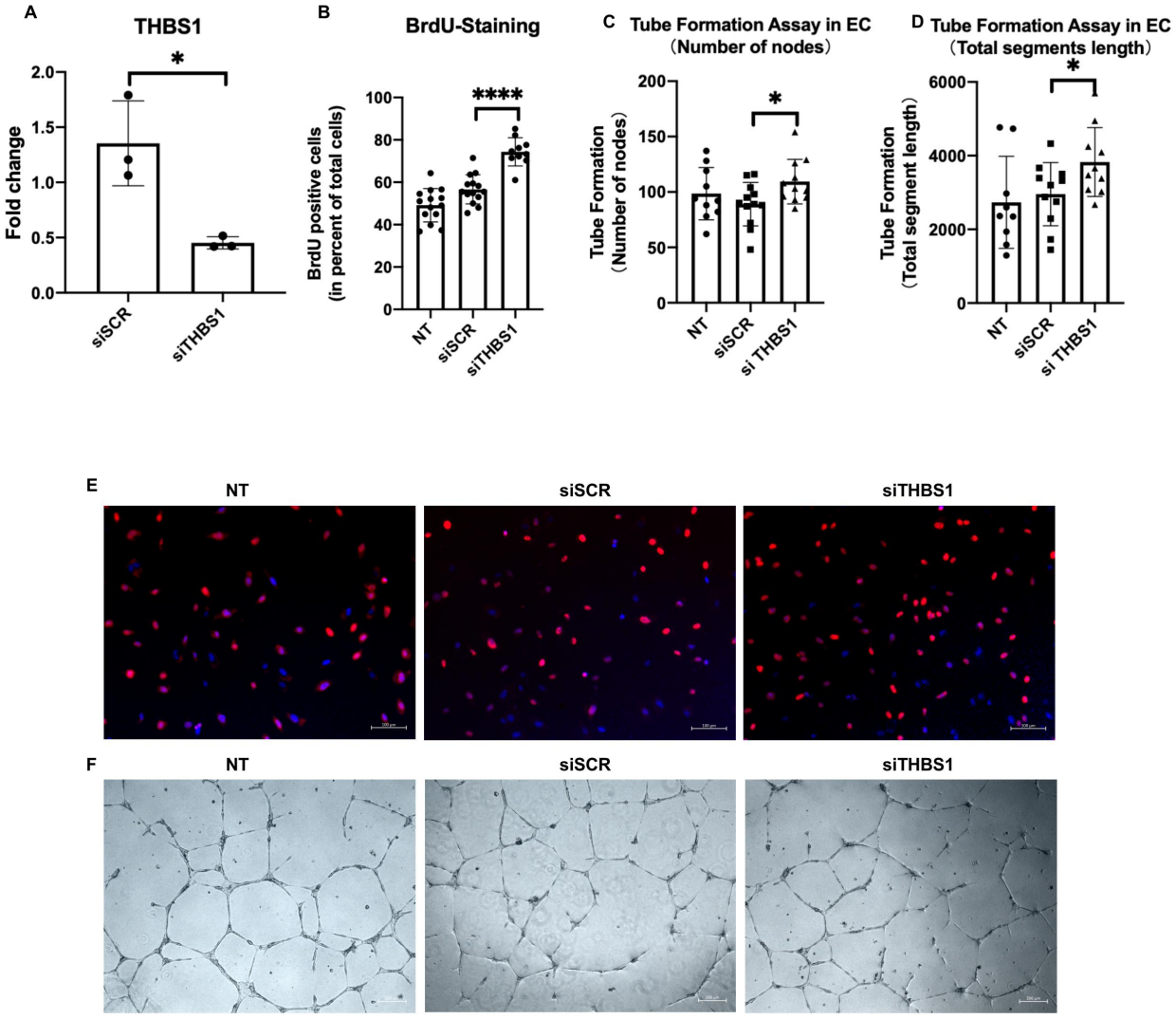

Fig. 6: THBS1 negatively regulates tube formation and proliferation in ECs. (A) siRNA was used to downregulate THBS1 expression in ECs, and the efficiency of HIF1a-AS1 knockdown was confirmed by qRT-PCR (*p < 0.05, n = 3, by student's t test). (B and E) BrdU incorporation was assessed by immunofluorescence (red) and nuclei were counterstained with DAPI (blue). The percentage of BrdU-positive cells was determined by calculating the ratio of BrdU-positive cells to the total number of cells (****P<0.0001, n = 10, by 1-way ANOVA with Bonferroni multiple comparisons test). The images were captured using a microscope at a magnification of 100× with a scale bar of 100 μm. In this BrdU assay, siTHBS1 demonstrated a significantly higher number of BrdU-positive cells in comparison to siSCR. (C and D and F) Tube formation assays were performed using ECs and the total length of the capillary tubes and node number were analyzed using ImageJ image analysis software (*p < 0.05, n > 6, by 1-way ANOVA with Bonferroni multiple comparisons test). The images were captured using a microscope at a magnification of 100× with a scale bar of 200 μm. In the tube formation assay, siTHBS1 exhibited higher values for both node number and total segment length than siSCR.

3.6 HIF1a-AS1 may regulates HIF1a transcription

We have previously established that HIF1a-AS1 plays a role in regulating THBS1 transcription and translation in ECs. Furthermore, it is widely accepted that HIF1a is a key player in promoting angiogenesis, while HIF1a-AS1 is known to act as a negative regulator of HIF1a. Nevertheless, the precise mechanisms through which HIF1a-AS1 governs the interplay between THBS1 and HIF1a remain somewhat enigmatic.

One potential mechanism by which HIF1a-AS1 can regulate gene expression is through post-transcriptional modulation of mRNA levels, notably mRNA stabilization. To investigate this possibility, we treated ECs with actinomycin D (ACTD, 5 µg/mL) to inhibit RNA synthesis and evaluated the expression of THBS1 and HIF1a using qRT-PCR after silencing HIF1a-AS1 under normoxic conditions. Our results indicated that silencing HIF1a-AS1 led to a downregulation of HIF1a transcript expression, while having a comparatively modest impact on the stability of THBS1 (Figure 7A-C). These findings suggest that HIF1a-AS1 may regulate HIF1a transcription under normoxic conditions, providing insights into the regulatory mechanism of HIF1a-AS1 on THBS1 expression. However, further investigations are required to determine the exact mechanism by which HIF1a-AS1 regulates HIF1a transcription.

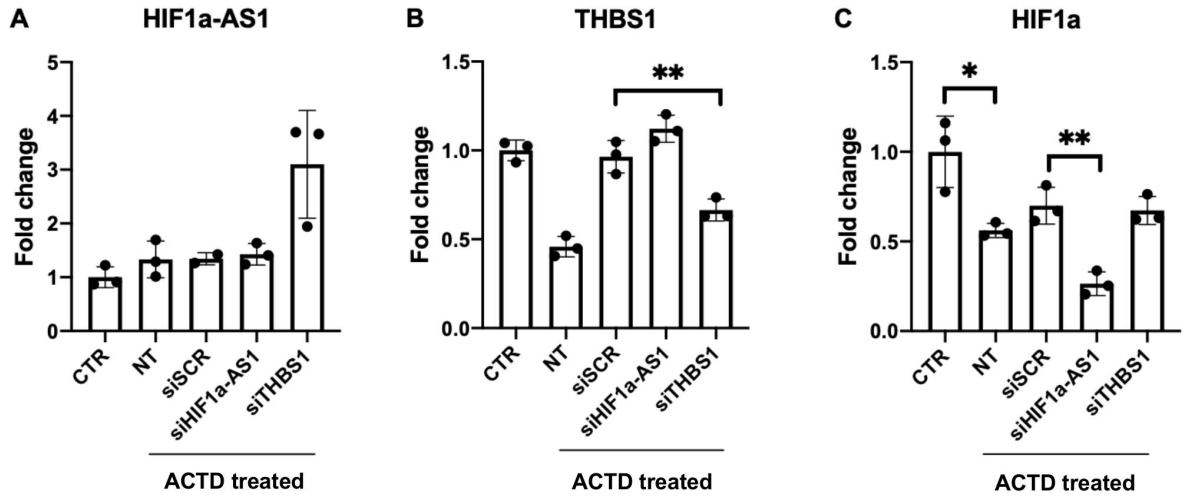

Fig. 7: HIF1a-AS1 could post-transcriptionally regulate mRNA levels by modulating mRNA stability. The stability of mRNA by using actinomycin D (ACTD) treatment (5 mg/mL for 24 hours) upon siRNA knockdown of HIF1a-AS1 or THBS1 or a scramble for 48 hours. The expression of (A) HIF1a-AS1 or (B) THBS1 or (C) HIF1a mRNAs was analyzed by

qRT-PCR in Ecs after siRNA treatment (*p < 0.5, **p < 0.1, n = 3, by 1-way ANOVA with Bonferroni multiple comparisons test).

3.7 Interaction of HIF1a-AS1 and THBS1 may contribute to EndMT

EndMT is a critical pathological process that has significant implications for the development of condition such as AVS and CAD. Our prior investigations has revealed the substantial involvement of HIF1a-AS1 in regulating EC proliferation and angiogenesis. In light of these findings, our current study sought to delve deeper into the roles of HIF1a-AS1 and THBS1 in the context of EndMT.

Firstly, to examine EndMT *in vitro*, ECs were treated with TGFβ+IL1β or TNF-α for 5 days, and the results showed that EndMT was successfully induced, as indicated by the downregulation of endothelial markers (von Willebrand factor [vWF], endothelial nitric oxide synthase [eNOS]) and the upregulation of mesenchymal markers (aSMA, smooth muscle [SM22]) (Figure 8A-B).

Our subsequent inquiry centered on deciphering the specific role of HIF1a-AS1 in the context of EndMT. Surprisingly, our qRT-PCR analysis revealed that the expression of HIF1a-AS1 hardly changed compared to control during the course of EndMT induction in ECs (Figure 8C-D). However, interestingly, the protein level of THBS1 was found to be regulated by HIF1a-AS1 in a context-dependent manner. Specifically, THBS1 was downregulated in TNF-α induced EndMT after knockdown of HIF1a-AS1, whereas the protein level of THBS1 was upregulated in HIF1a-AS1-silenced cells in TGFβ and IL-1-induced EndMT (Figure 8E). These findings suggest that the interaction between HIF1a-AS1 and THBS1 may exert a pivotal influence on the complex process of EndMT.

Based on the experimental data, our study has revealed several significant findings about the roles and mechanisms of action of HIF1a-AS1 and HIF1a-AS2 in ECs. Specifically, HIF1a-AS1 was shown to have anti-angiogenic and anti-proliferative effects, and may regulate THBS1 transcription and translation, which provides insights into the regulation of angiogenesis. Furthermore, we found that HIF1a-AS1 can be transferred from donor cells to recipient ECs via EVs, which may contribute to intercellular communication. On the other hand, HIF1a-AS2 was found to act as an anti-proliferation gene in ECs. Additionally, our results suggest that HIF1a-AS1 may also regulate HIF1a transcription under normoxic conditions and that the interaction between HIF1a-AS1 and THBS1 may

play a role in the EndMT process. Overall, these findings highlight the complex regulatory network involved in angiogenesis and provide potential targets for therapeutic intervention.

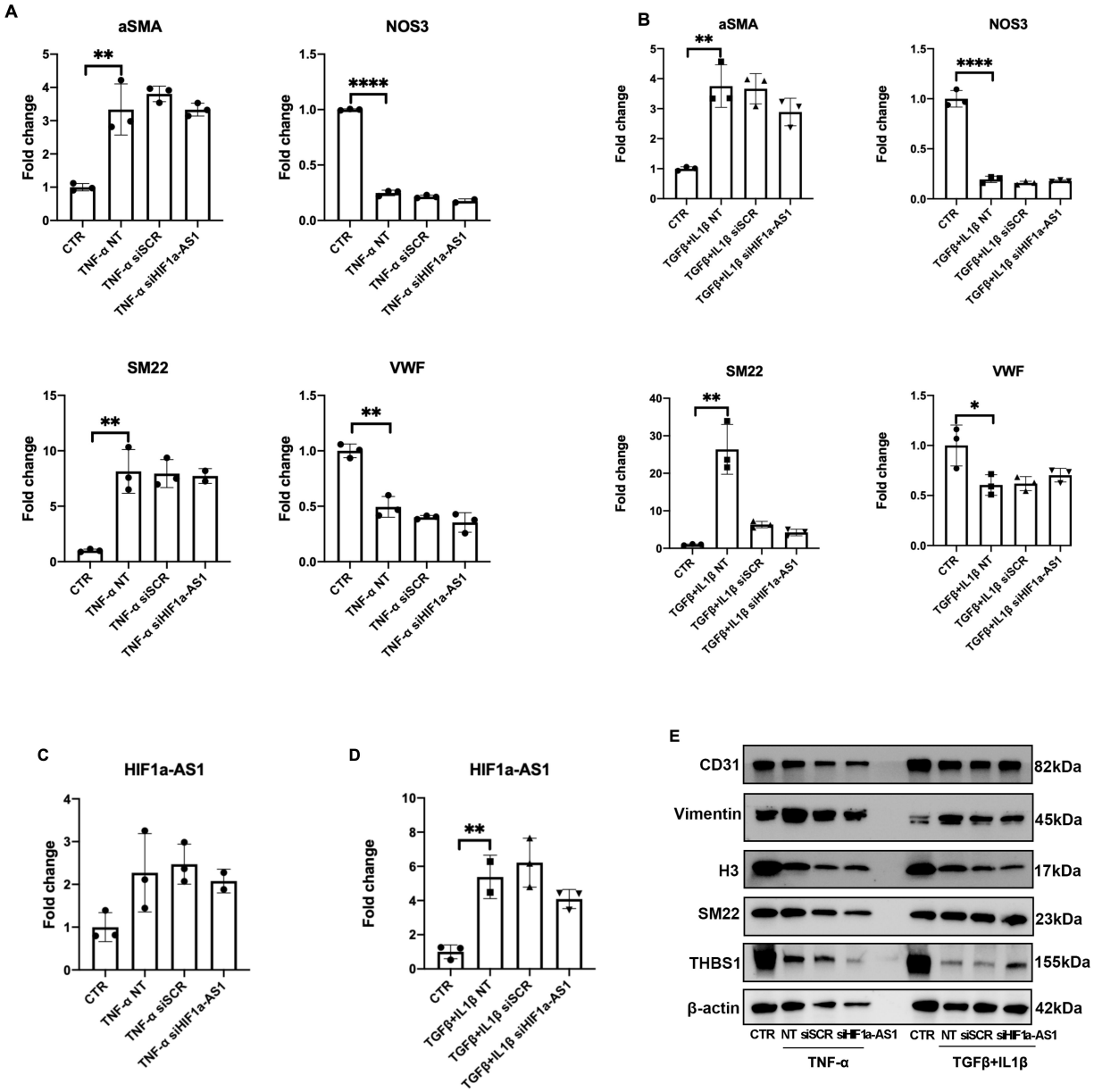

Fig. 8: The effect of HIF1a-AS1 knockdown on endothelial to mesenchymal transition (EndMT) of HUVECs. Tumor necrosis factor alpha (TNF-α), transforming growth factor beta (TGFβ) and interleukin-1β (IL1β) induced EndMT in ECs. ECs were transfected with HIF1a-AS1 siRNA and siSCR (n = 3) for 48 h, then ECs were treated with TNF-α or TGFβ+IL1β for 5 days. (A and B) The endothelial marker (von Willebrand factor [vWF], endothelial nitric oxide synthase [eNOS]) and mesenchymal marker (a-smooth muscle actin [aSMA], smooth muscle [SM22]) expression were assessed by qRT-PCR (n = 3, **P < 0.01, ****P < 0.0001, by Student's t test). (C and D) The HIF1a-AS1 levels were determined after treating with TNF-α or TGFβ+IL1β for 5 days by qRT-PCR (n = 3, **P < 0.01, by Student's t test). (E) Endothelial marker (CD31) and mesenchymal marker (SM22,

Vimentin) and THBS1 protein levels were assessed by Western blot in ECs that were transfected with HIF1a-AS1 siRNA and siSCR. H3 and β-Actin were used as the loading control.

4. Discussion

In patients with AVS, there is no pharmacotherapy to prevent aortic valve calcification, and the urgency to replace the valve to relieve symptoms and reduce cardiac burden is still associated with high morbidity and mortality (Nightingale, et al., 2005, Makkar, et al., 2012). To date, the biological or physiological differences in the AVS patients have not been extensively studied, so it is necessary to discover the new mechanism and treatment to intervene in the progression of the AVS.

LncRNAs have been identified as both biomarkers and regulators of CVDs. For instance, the expression levels of lncRNA H19 have been associated with CAD (Liu, et al., 2016, Xiong, et al., 2019). In addition, it has been reported that lncRNA H19 plays a role in the protective effects of EVs released by adipose tissue-derived mesenchymal stem cells (ATV-MSC-exos) on regulating angiogenesis and promoting the healing of myocardial damage. On the other hand, lncRNA H19 has also been found to increase in CAVD, promoting an osteogenic program by affecting NOTCH1 expression (Huang, et al., 2020). These findings underscore the potential of lncRNAs as targets for therapeutic intervention in CVDs.

In our recent study, we conducted a PCR-based human lncRNA array on a screening cohort comprising patients with stable CAD and non-CAD (NCAD) to identify potential biomarkers. We found that the lncRNA HIF1a-AS1 was significantly upregulated in CAD patients (Hosen, et al., 2021). Given that both AVS and CAD are types of atherosclerotic disease and share similar risk factors, AVS can be regarded as a surrogate marker for cardiovascular events related to CAD. Therefore, we aimed to investigate whether they share a common underlying mechanism.

The lncRNA HIF1a-AS1 is located on the antisense strand of HIF1a and is markedly dysregulated in both ECs and CVDs. Recent studies have shown that the levels of exosomes and the exosomal lncRNA HIF1a-AS1 are significantly higher in patients with atherosclerosis, and there is a positive correlation between them. Therefore, exosomes and exosomal lncRNA HIF1a-AS1 could potentially serve as biomarkers for atherosclerosis (Wang, et al., 2017). HIF1a-AS1 has been reported to regulate endothelial function and is significantly increased in patients with CAD and AVS (Wang, et al., 2015,

Hosen, et al., 2021, Gong, et al., 2022). Recent studies suggest that oxLDL and TNF-α are key players in the development of atherosclerosis and endothelial dysfunction, and they are commonly used as stimuli to induce these conditions *in vitro* and *in vivo* (Li, et al., 2005, Zhang, et al., 2006, Sitia, et al., 2010). In line with our clinical findings and related studies, our *in vitro* experiments showed that HIF1a-AS1 levels increased in a dose-dependent manner when ECs were stimulated with oxLDL and TNF-α at concentrations of 10 ng/mL and 20 ng/mL, respectively. However, higher concentrations, such as 50 ng/mL, resulted in the death of most cells. Additionally, we observed the transfer of HIF1a-AS1-silencing flow from EVs or EC with HIF1a-AS1 transfection to normal target ECs. However, the media involved in this intercellular transfer of the HIF1a-AS1-silencing flow remains to be further investigated. Overall, our findings suggest that HIF1a-AS1 may contribute to the development of atherosclerosis and endothelial dysfunction, and EVs have the potential to transfer HIF1a-AS1 from donor cells to recipient ECs. Further research is needed to understand the underlying mechanisms of its effects.

HIF1a-AS1 is a gene with relevance to disease, as it has been implicated in endothelial dysfunction and vascularization (Yu, et al., 2018). Another natural antisense transcript of HIF1a, HIF1a-AS2, which originates from the 3' region of the HIF1a gene and binds to HIF1a mRNA 3' untranslated region, has also been shown to be highly expressed in atherosclerotic mice and involved in the proliferation and migration of aortic smooth muscle cells in aortic dissection (Li, et al., 2020, Zhang, et al., 2022). In our study, we sought to investigate the specific roles of HIF1a-AS1 and HIF1a-AS2 in endothelial cell biology and cardiovascular disease. Our functional *in vitro* experiments showed that HIF1a-AS1 negatively regulates endothelial cell proliferation and vascular tube formation, which are key processes in angiogenesis. Similarly, HIF1a-AS2 was found to negatively regulate endothelial cell proliferation, but there was no significant change in tube formation compared with the scramble group. These findings differ from those reported by Li et al., who showed that HIF1a-AS2 promotes angiogenesis in endothelial cells under hypoxia by sponging miR-153-3p and upregulating HIF1a (Li, et al., 2017). The discrepancy could be due to differences in the oxygen levels of the cells in the different experiments.

HIF1a-AS1 has been shown to regulate angiogenesis and target multiple genes, including miR-138 and let-7g (Huang, et al., 2020, Zhang, et al., 2020). In our study, we found that silencing HIF1a-AS1 in ECs led to downregulation of several genes, including THBS1,

NRP1, AKT1, etc., as revealed by a PCR-based gene expression array. However, single real-time PCR experiments showed that only THBS1 was upregulated. To investigate the discrepancy between the array and PCR results, we examined THBS1 protein expression after HIF1a-AS1 knockdown by Western blot and immunofluorescence staining, and observed a downregulation of THBS1 expression in HIF1a-AS1-silenced cells. This suggests that HIF1a-AS1 may regulate THBS1 translation, which is different from the RNA level. This paradoxical effect may be due to post-transcriptional regulation, transcriptional degradation, posttranslational processing, or modification, as has been reported previously (Kors, et al., 2019).

Based on the experimental results, it appears that the gene HIF1a-AS1 is involved in the development of atherosclerosis and inhibits angiogenesis. Similarly, HIF1a-AS2 was observed to negatively impact endothelial cell proliferation. Inhibition of HIF1a-AS1 at the RNA level leads to an increase in THBS1 mRNA expression, which is an inhibitor of angiogenesis. However, at the protein level, THBS1 expression is decreased, which could promote angiogenesis.

HIF1a has been found to play a role in atherosclerotic lesions and has been associated with endothelial dysfunction, inflammation, macrophage proliferation, and smooth muscle cell growth (Semenza, 2014). It has also been shown to induce angiogenesis in ischemic tissue, as seen in previous studies (Kelly, et al., 2003). To investigate the possibility of HIF1a-AS1 post-transcriptionally regulating mRNA levels by modulating mRNA stability and/or accelerating the process of target message decay, we treated cells with ACTD and CHX under normoxic conditions to inhibit RNA synthesis and analyzed the expression profile of HIF1a and THBS1 using qRT-PCR. Our results showed that the downregulation of HIF1a transcript was observed in HIF1a-AS1-silenced cells, indicating that HIF1a-AS1 could regulate HIF1a transcription. However, we found no significant changes in the mRNA levels of THBS1. Overall, our findings suggest a potential role of HIF1a-AS1 in regulating HIF1a transcription and provide insights into the mechanisms underlying the regulation of angiogenesis.

Furthermore, to further explore the potential involvement of HIF1a-AS1 in AVS or CAD, we investigated EndMT in vitro, which is a complex cellular transdifferentiation process whereby endothelial cells lose their endothelial identity and acquire mesenchymal cell characteristics (Kovacic, et al., 2019). We induced EndMT in vitro by subjecting ECs to

TNF-α or TGFβ+IL1β for 5 days and characterized its molecular signature using RT-qPCR. Although we observed a successful induction of EndMT, RT-PCR analysis revealed no significant changes in HIF1a-AS1 expression after five days of treatment with either TNF-α or TGFβ+IL1β. The lack of change in HIF1a-AS1 expression may be due to high cell density or low siRNA stability. To further investigate the role of HIF1a-AS1, we evaluated the protein content of our target gene using Western blot analysis. Successful induction of EndMT was confirmed, and we observed that the protein content of THBS1 differed between TNF-α and TGFβ+IL1β treatment in the HIF1a-AS1-silenced group. Interestingly, THBS1 protein expression was opposite after TGFβ+IL1β treatment, suggesting that THBS1 may be involved in a TGFβ-related signaling pathway that influences its expression (Sun, et al., 2022). This pathway may be the reason for the differential expression of THBS1 under TGFβ- and IL-1β-induced and TNF-α-induced EndMT. Furthermore, previous studies have reported that TGFβ signaling plays a direct role in controlling THBS1 transcriptional activity via SMAD3 (Daubon, et al., 2019).

Nevertheless, our study has some limitations that need to be addressed in future research: (i) The underlying mechanism of HIF1a-AS1-mediated intercellular communication needs further investigation to fully understand its regulatory role in angiogenesis. (ii) Additional research on the molecular mechanism of HIF1a-AS1 in cardiovascular cells, such as cardiomyocytes or valvular interstitial cells, or in animal models, such as the murine model, is necessary to confirm our findings. (iii) Further investigation into the function of HIF1a-AS1 in regulating HIF1a under hypoxia will provide valuable insights into the regulation of lncRNAs in AVS.

In conclusion, our study provides new mechanistic insights into the role of lncRNA in the regulation of angiogenesis in AVS: (1) two independent atherosclerotic stimuli (oxLDL and TNF-α) upregulate the expression of HIF1a-AS1 in ECs; (2) HIF1a-AS1 regulates EC function by controlling the expression of THBS1, a negative regulator of EC angiogenesis, and stabilizing HIF1a; (3) Successful induction of EndMT in ECs suggests that the interaction between HIF1a-AS1 and THBS1 may play a role in EndMT. Future investigation into the underlying mechanism of HIF1a-AS1-mediated regulation of the angiogenic gene network in AVS will further advance our understanding of the role of lncRNAs in AVS.

5. Summary

In this study, we aimed to investigate the specific role of long noncoding HIF1a antisense RNA 1 (HIF1a-AS1) in Cardiovascular diseases (CVDs), with a specific focus on its implications for aortic valve stenosis (AVS). Atherosclerotic stimuli could upregulate the expression of HIF1a-AS1, and knockdown of HIF1a-AS1 in endothelial cells (ECs) increased their effects on cellular function (proliferation, tube formation, angiogenesis). Besides, loss of HIF1a-AS1 promotes Thrombospondin 1 (THBS1) mRNA and inhibits protein expression. Furthermore, the study identified potential Extracellular Vesicles (EV) mediated transfer of HIF1a-AS1 between cells. Notably, the protein THBS1 exhibited distinct regulation upon Endothelial-to-mesenchymal transition (EndMT) depending on HIF1a-AS1 levels.

These findings demonstrate that HIF1a-AS1 regulates ECs function via a THBS1-dependent mechanism. HIF1a-AS1 may regulate protein expression of THBS1 in endothelial cells under EndMT. The role of endothelial dysfunction and EndMT in the pathogenesis of AVS is increasingly recognized. Understanding how HIF1a-AS1 regulates THBS1 in the context of EndMT offers insights into the cellular processes driving valve remodeling in AVS. Modulating HIF1a-AS1 levels or its downstream signaling pathways may help mitigate the progression of AVS, particularly by preventing or reversing endothelial dysfunction and EndMT-related changes.

In conclusion, this research has the potential to advance our understanding of the disease, facilitate the development of targeted therapies, and ultimately benefit patients suffering from AVS.

6. List of figures

7. List of tables

8. References

Aikawa E, Nahrendorf M, Sosnovik D, Lok VM, Jaffer FA, Aikawa M, Weissleder R. Multimodality molecular imaging identifies proteolytic and osteogenic activities in early aortic valve disease. Circulation 2007; 115: 377-386

Aikawa E, Whittaker P, Farber M, Mendelson K, Padera RF, Aikawa M, Schoen FJ. Human semilunar cardiac valve remodeling by activated cells from fetus to adult: implications for postnatal adaptation, pathology, and tissue engineering. Circulation 2006; 113: 1344-1352

Benjamin EJ, Muntner P, Alonso A, Bittencourt MS, Callaway CW, Carson AP, Chamberlain AM, Chang AR, Cheng S, Das SR, Delling FN, Djousse L, Elkind MSV, Ferguson JF, Fornage M, Jordan LC, Khan SS, Kissela BM, Knutson KL, Kwan TW, Lackland DT, Lewis TT, Lichtman JH, Longenecker CT, Loop MS, Lutsey PL, Martin SS, Matsushita K, Moran AE, Mussolino ME, O'Flaherty M, Pandey A, Perak AM, Rosamond WD, Roth GA, Sampson UKA, Satou GM, Schroeder EB, Shah SH, Spartano NL, Stokes A, Tirschwell DL, Tsao CW, Turakhia MP, VanWagner LB, Wilkins JT, Wong SS, Virani SS. Heart Disease and Stroke Statistics-2019 Update: A Report From the American Heart Association. Circulation 2019; 139: e56-e528

Butcher JT, Mahler GJ, Hockaday LA. Aortic valve disease and treatment: the need for naturally engineered solutions. Adv Drug Deliv Rev 2011; 63: 242-268

Chen D, Wu L, Liu L, Gong Q, Zheng J, Peng C, Deng J. Comparison of HIF1A-AS1 and HIF1A-AS2 in regulating HIF-1α and the osteogenic differentiation of PDLCs under hypoxia. Int J Mol Med 2017; 40: 1529-1536

Chen PY, Schwartz MA, Simons M. Endothelial-to-Mesenchymal Transition, Vascular Inflammation, and Atherosclerosis. Front Cardiovasc Med 2020; 7: 53

Chen YG, Kim MV, Chen X, Batista PJ, Aoyama S, Wilusz JE, Iwasaki A, Chang HY. Sensing Self and Foreign Circular RNAs by Intron Identity. Mol Cell 2017; 67: 228-238.e225

Combs MD, Yutzey KE. Heart valve development: regulatory networks in development and disease. Circ Res 2009; 105: 408-421

Cyr AR, Huckaby LV, Shiva SS, Zuckerbraun BS. Nitric Oxide and Endothelial Dysfunction. Crit Care Clin 2020; 36: 307-321

Daubon T, Léon C, Clarke K, Andrique L, Salabert L, Darbo E, Pineau R, Guérit S, Maitre M, Dedieu S, Jeanne A, Bailly S, Feige JJ, Miletic H, Rossi M, Bello L, Falciani F, Bjerkvig RBikfalvi A. Deciphering the complex role of thrombospondin-1 in glioblastoma development. Nat Commun 2019; 10: 1146

Evrard SM, Lecce L, Michelis KC, Nomura-Kitabayashi A, Pandey G, Purushothaman KR, Escamard V, Li JR, Hadri L, Fujitani K, Moreno PR, Benard L, Rimmele P, Cohain A, Mecham B, Randolph GJ, Nabel EG, Hajjar R, Fuster V, Boehm M, Kovacic JC. Endothelial to mesenchymal transition is common in atherosclerotic lesions and is associated with plaque instability. Nat Commun 2016; 7: 11853

Furman C, Copin C, Kandoussi M, Davidson R, Moreau M, Taggiart F, Chapman MJ, Fruchart JC, Rouis M. Rosuvastatin reduces MMP-7 secretion by human monocyte-derived macrophages: potential relevance to atherosclerotic plaque stability. Atherosclerosis 2004; 174: 93-98

Gan L, Xie D, Liu J, Bond Lau W, Christopher TA, Lopez B, Zhang L, Gao E, Koch W, Ma XLWang Y. Small Extracellular Microvesicles Mediated Pathological Communications Between Dysfunctional Adipocytes and Cardiomyocytes as a Novel Mechanism Exacerbating Ischemia/Reperfusion Injury in Diabetic Mice. Circulation 2020; 141: 968-983

Gong Z, Yang J, Dong J, Li H, Wang B, Du K, Zhang C, Chen L. LncRNA HIF1A-AS1 Regulates the Cellular Function of HUVECs by Globally Regulating mRNA and miRNA Expression. Front Biosci 2022; 27: 330

Hansson GK, Hermansson A. The immune system in atherosclerosis. Nat Immunol 2011; 12: 204-212

Holdt LM, Stahringer A, Sass K, Pichler G, Kulak NA, Wilfert W, Kohlmaier A, Herbst A, Northoff BH, Nicolaou A, Gäbel G, Beutner F, Scholz M, Thiery J, Musunuru K, Krohn K, Mann M, Teupser D. Circular non-coding RNA ANRIL modulates ribosomal RNA maturation and atherosclerosis in humans. Nat Commun 2016; 7: 12429

Hosen MR, Goody PR, Zietzer A, Xiang X, Niepmann ST, Sedaghat A, Tiyerili V, Chennupati R, Moore JBt, Boon RA, Uchida S, Sinning JM, Zimmer S, Latz E, Werner N, Nickenig G, Jansen F. Circulating MicroRNA-122-5p Is Associated With a Lack of Improvement in Left Ventricular Function After Transcatheter Aortic Valve Replacement and Regulates Viability of Cardiomyocytes Through Extracellular Vesicles. Circulation 2022; 146: 1836-1854

Hosen MR, Li Q, Liu Y, Zietzer A, Maus K, Goody P, Uchida S, Latz E, Werner N, Nickenig G, Jansen F. CAD increases the long noncoding RNA PUNISHER in small extracellular vesicles and regulates endothelial cell function via vesicular shuttling. Mol Ther Nucleic Acids 2021; 25: 388-405

Huang P, Wang L, Li Q, Tian X, Xu J, Xu J, Xiong Y, Chen G, Qian H, Jin C, Yu Y, Cheng K, Qian L, Yang Y. Atorvastatin enhances the therapeutic efficacy of mesenchymal stem cells-derived exosomes in acute myocardial infarction via up-regulating long non-coding RNA H19. Cardiovasc Res 2020; 116: 353-367

Ishii N, Ozaki K, Sato H, Mizuno H, Susumu S, Takahashi A, Miyamoto Y, Ikegawa S, Kamatani N, Hori M, Satoshi S, Nakamura Y, Tanaka T. Identification of a novel non-coding RNA, MIAT, that confers risk of myocardial infarction. J Hum Genet 2006; 51: 1087-1099

Kaikkonen MU, Lam MT, Glass CK. Non-coding RNAs as regulators of gene expression and epigenetics. Cardiovasc Res 2011; 90: 430-440

Kelly BD, Hackett SF, Hirota K, Oshima Y, Cai Z, Berg-Dixon S, Rowan A, Yan Z, Campochiaro PA, Semenza GL. Cell type-specific regulation of angiogenic growth factor

gene expression and induction of angiogenesis in nonischemic tissue by a constitutively active form of hypoxia-inducible factor 1. Circ Res 2003; 93: 1074-1081

Kors S, Geijtenbeek K, Reits E, Schipper-Krom S. Regulation of Proteasome Activity by (Post-)transcriptional Mechanisms. Front Mol Biosci 2019; 6: 48

Kovacic JC, Dimmeler S, Harvey RP, Finkel T, Aikawa E, Krenning G, Baker AH. Endothelial to Mesenchymal Transition in Cardiovascular Disease: JACC State-of-the-Art Review. J Am Coll Cardiol 2019; 73: 190-209

Kumarswamy R, Bauters C, Volkmann I, Maury F, Fetisch J, Holzmann A, Lemesle G, Groote P, Pinet F, Thum T. Circulating long noncoding RNA, LIPCAR, predicts survival in patients with heart failure. Circ Res 2014; 114: 1569-1575

Li D, Mehta JL. Oxidized LDL, a critical factor in atherogenesis. Cardiovasc Res 2005; 68: 353-354

Li L, Wang M, Mei Z, Cao W, Yang Y, Wang Y, Wen A. lncRNAs HIF1A-AS2 facilitates the up-regulation of HIF-1α by sponging to miR-153-3p, whereby promoting angiogenesis in HUVECs in hypoxia. Biomed Pharmacother 2017; 96: 165-172

Li P, Xing J, Zhang J, Jiang J, Liu X, Zhao D, Zhang Y. Inhibition of long noncoding RNA HIF1A-AS2 confers protection against atherosclerosis via ATF2 downregulation. J Adv Res 2020; 26: 123-135

Libby P. Mechanisms of acute coronary syndromes and their implications for therapy. N Engl J Med 2013; 368: 2004-2013

Libby P. The changing landscape of atherosclerosis. Nature 2021; 592: 524-533

Libby P, Ridker PMHansson GK. Progress and challenges in translating the biology of atherosclerosis. Nature 2011; 473: 317-325

Liebner S, Cattelino A, Gallini R, Rudini N, Iurlaro M, Piccolo S, Dejana E. Beta-catenin is required for endothelial-mesenchymal transformation during heart cushion development in the mouse. J Cell Biol 2004; 166: 359-367

Liu L, An X, Li Z, Song Y, Li L, Zuo S, Liu N, Yang G, Wang H, Cheng X, Zhang Y, Yang X, Wang J. The H19 long noncoding RNA is a novel negative regulator of cardiomyocyte hypertrophy. Cardiovasc Res 2016; 111: 56-65

Liu Y, Li Q, Hosen MR, Zietzer A, Flender A, Levermann P, Schmitz T, Frühwald D, Goody P, Nickenig G, Werner N, Jansen F. Atherosclerotic Conditions Promote the Packaging of Functional MicroRNA-92a-3p Into Endothelial Microvesicles. Circ Res 2019; 124: 575-587

Mahler GJ, Farrar EJ, Butcher JT. Inflammatory cytokines promote mesenchymal transformation in embryonic and adult valve endothelial cells. Arterioscler Thromb Vasc Biol 2013; 33: 121-130

Makkar RR, Fontana GP, Jilaihawi H, Kapadia S, Pichard AD, Douglas PS, Thourani VH, Babaliaros VC, Webb JG, Herrmann HC, Bavaria JE, Kodali S, Brown DL, Bowers B, Dewey TM, Svensson LG, Tuzcu M, Moses JW, Williams MR, Siegel RJ, Akin JJ, Anderson WN, Pocock S, Smith CR, Leon MB. Transcatheter aortic-valve replacement for inoperable severe aortic stenosis. N Engl J Med 2012; 366: 1696-1704

Manduteanu I, Popov D, Radu A, Simionescu M. Calf cardiac valvular endothelial cells in culture: production of glycosaminoglycans, prostacyclin and fibronectin. J Mol Cell Cardiol 1988; 20: 103-118

Mohler ER, Gannon F, Reynolds C, Zimmerman R, Keane MG, Kaplan FS. Bone formation and inflammation in cardiac valves. Circulation 2001; 103: 1522-1528

Nigam V, Srivastava D. Notch1 represses osteogenic pathways in aortic valve cells. J Mol Cell Cardiol 2009; 47: 828-834

Nightingale AK, Horowitz JD. Aortic sclerosis: not an innocent murmur but a marker of increased cardiovascular risk. Heart 2005; 91: 1389-1393

Palazzo AF, Lee ES. Non-coding RNA: what is functional and what is junk? Front Genet 2015; 6: 2

Paranya G, Vineberg S, Dvorin E, Kaushal S, Roth SJ, Rabkin E, Schoen FJ, Bischoff J. Aortic valve endothelial cells undergo transforming growth factor-beta-mediated and non-

transforming growth factor-beta-mediated transdifferentiation in vitro. Am J Pathol 2001; 159: 1335-1343

Patil VS, Zhou RR. Gene regulation by non-coding RNAs. Crit Rev Biochem Mol Biol 2014; 49: 16-32

Poller W, Dimmeler S, Heymans S, Zeller T, Haas J, Karakas M, Leistner DM, Jakob P, Nakagawa S, Blankenberg S, Engelhardt S, Thum T, Weber C, Meder B, Hajjar RL, Messer U. Non-coding RNAs in cardiovascular diseases: diagnostic and therapeutic perspectives. Eur Heart J 2018; 39: 2704-2716

Rajamannan NM. Calcific aortic valve disease: cellular origins of valve calcification. Arterioscler Thromb Vasc Biol 2011; 31: 2777-2778

Rajamannan NM, Subramaniam M, Rickard D, Stock SR, Donovan J, Springett M, Orszulak T, Fullerton DA, Tajik AJ, Bonow ROSpelsberg T. Human aortic valve calcification is associated with an osteoblast phenotype. Circulation 2003; 107: 2181-2184

Rodríguez-Lorenzo S, Ferreira Francisco DM, Vos R, van Het Hof B, Rijnsburger M, Schroten H, Ishikawa H, Beaino W, Bruggmann R, Kooij Gde Vries HE. Altered secretory and neuroprotective function of the choroid plexus in progressive multiple sclerosis. Acta Neuropathol Commun 2020; 8: 35

GBD 2017 Causes of Death Collaborators. Global, regional, and national age-sex-specific mortality for 282 causes of death in 195 countries and territories, 1980-2017: a systematic analysis for the Global Burden of Disease Study 2017. Lancet 2018; 392: 1736-1788

Salim MT, Villa-Roel N, Vogel B, Jo H, Yoganathan AP. HIF1A inhibitor PX-478 reduces pathological stretch-induced calcification and collagen turnover in aortic valve. Front Cardiovasc Med 2022; 9: 1002067

Schneider F, Sukhova GK, Aikawa M, Canner J, Gerdes N, Tang SM, Shi GP, Apte SS, Libby P. Matrix-metalloproteinase-14 deficiency in bone-marrow-derived cells promotes collagen accumulation in mouse atherosclerotic plaques. Circulation 2008; 117: 931-939

Semenza GL. Oxygen sensing, hypoxia-inducible factors, and disease pathophysiology. Annu Rev Pathol 2014; 9: 47-71

Siney L, Lewis MJ. Nitric oxide release from porcine mitral valves. Cardiovasc Res 1993; 27: 1657-1661

Sitia S, Tomasoni L, Atzeni F, Ambrosio G, Cordiano C, Catapano A, Tramontana S, Perticone F, Naccarato P, Camici P, Picano E, Cortigiani L, Bevilacqua M, Milazzo L, Cusi D, Barlassina C, Sarzi-Puttini P, Turiel M. From endothelial dysfunction to atherosclerosis. Autoimmun Rev 2010; 9: 830-834

Sun J, Ge X, Wang Y, Niu L, Tang L, Pan S. USF2 knockdown downregulates THBS1 to inhibit the TGF-β signaling pathway and reduce pyroptosis in sepsis-induced acute kidney injury. Pharmacol Res 2022; 176: 105962

Tabas I. Macrophage death and defective inflammation resolution in atherosclerosis. Nat Rev Immunol 2010; 10: 36-46

Théry C, Witwer KW, Aikawa E, Alcaraz MJ, Anderson JD, Andriantsitohaina R, Antoniou A, Arab T, Archer F, Atkin-Smith GK, Ayre DC, Bach JM, Bachurski D, Baharvand H, Balaj L, Baldacchino S, Bauer NN, Baxter AA, Bebawy M, Beckham C, Bedina Zavec A, Benmoussa A, Berardi AC, Bergese P, Bielska E, Blenkiron C, Bobis-Wozowicz S, Boilard E, Boireau W, Bongiovanni A, Borràs FE, Bosch S, Boulanger CM, Breakefield X, Breglio AM, Brennan M, Brigstock DR, Brisson A, Broekman ML, Bromberg JF, Bryl-Górecka P, Buch S, Buck AH, Burger D, Busatto S, Buschmann D, Bussolati B, Buzás EI, Byrd JB, Camussi G, Carter DR, Caruso S, Chamley LW, Chang YT, Chen C, Chen S, Cheng L, Chin AR, Clayton A, Clerici SP, Cocks A, Cocucci E, Coffey RJ, Cordeiro-da-Silva A, Couch Y, Coumans FA, Coyle B, Crescitelli R, Criado MF, D'Souza-Schorey C, Das S, Datta Chaudhuri A, de Candia P, De Santana EF, De Wever O, Del Portillo HA, Demaret T, Deville S, Devitt A, Dhondt B, Di Vizio D, Dieterich LC, Dolo V, Dominguez Rubio AP, Dominici M, Dourado MR, Driedonks TA, Duarte FV, Duncan HM, Eichenberger RM, Ekström K, El Andaloussi S, Elie-Caille C, Erdbrügger U, Falcón-Pérez JM, Fatima F, Fish JE, Flores-Bellver M, Försönits A, Frelet-Barrand A, Fricke F, Fuhrmann G, Gabrielsson S, Gámez-Valero A, Gardiner C, Gärtner K, Gaudin R, Gho YS, Giebel B, Gilbert C,

Gimona M, Giusti I, Goberdhan DC, Görgens A, Gorski SM, Greening DW, Gross JC, Gualerzi A, Gupta GN, Gustafson D, Handberg A, Haraszti RA, Harrison P, Hegyesi H, Hendrix A, Hill AF, Hochberg FH, Hoffmann KF, Holder B, Holthofer H, Hosseinkhani B, Hu G, Huang Y, Huber V, Hunt S, Ibrahim AG, Ikezu T, Inal JM, Isin M, Ivanova A, Jackson HK, Jacobsen S, Jay SM, Jayachandran M, Jenster G, Jiang L, Johnson SM, Jones JC, Jong A, Jovanovic-Talisman T, Jung S, Kalluri R, Kano SI, Kaur S, Kawamura Y, Keller ET, Khamari D, Khomyakova E, Khvorova A, Kierulf P, Kim KP, Kislinger T, Klingeborn M, Klinke DJ, 2nd, Kornek M, Kosanović MM, Kovács Á F, Krämer-Albers EM, Krasemann S, Krause M, Kurochkin IV, Kusuma GD, Kuypers S, Laitinen S, Langevin SM, Languino LR, Lannigan J, Lässer C, Laurent LC, Lavieu G, Lázaro-Ibáñez E, Le Lay S, Lee MS, Lee YXF, Lemos DS, Lenassi M, Leszczynska A, Li IT, Liao K, Libregts SF, Ligeti E, Lim R, Lim SK, Linē A, Linnemannstöns K, Llorente A, Lombard CA, Lorenowicz MJ, Lörincz Á M, Lötvall J, Lovett J, Lowry MC, Loyer X, Lu Q, Lukomska B, Lunavat TR, Maas SL, Malhi H, Marcilla A, Mariani J, Mariscal J, Martens-Uzunova ES, Martin-Jaular L, Martinez MC, Martins VR, Mathieu M, Mathivanan S, Maugeri M, McGinnis LK, McVey MJ, Meckes DG, Jr., Meehan KL, Mertens I, Minciacchi VR, Möller A, Møller Jørgensen M, Morales-Kastresana A, Morhayim J, Mullier F, Muraca M, Musante L, Mussack V, Muth DC, Myburgh KH, Najrana T, Nawaz M, Nazarenko I, Nejsum P, Neri C, Neri T, Nieuwland R, Nimrichter L, Nolan JP, Nolte-'t Hoen EN, Noren Hooten N, O'Driscoll L, O'Grady T, O'Loghlen A, Ochiya T, Olivier M, Ortiz A, Ortiz LA, Osteikoetxea X, Østergaard O, Ostrowski M, Park J, Pegtel DM, Peinado H, Perut F, Pfaffl MW, Phinney DG, Pieters BC, Pink RC, Pisetsky DS, Pogge von Strandmann E, Polakovicova I, Poon IK, Powell BH, Prada I, Pulliam L, Quesenberry P, Radeghieri A, Raffai RL, Raimondo S, Rak J, Ramirez MI, Raposo G, Rayyan MS, Regev-Rudzki N, Ricklefs FL, Robbins PD, Roberts DD, Rodrigues SC, Rohde E, Rome S, Rouschop KM, Rughetti A, Russell AE, Saá P, Sahoo S, Salas-Huenuleo E, Sánchez C, Saugstad JA, Saul MJ, Schiffelers RM, Schneider R, Schøyen TH, Scott A, Shahaj E, Sharma S, Shatnyeva O, Shekari F, Shelke GV, Shetty AK, Shiba K, Siljander PR, Silva AM, Skowronek A, Snyder OL, 2nd, Soares RP, Sódar BW, Soekmadji C, Sotillo J, Stahl PD, Stoorvogel W, Stott SL, Strasser EF, Swift S, Tahara H, Tewari M, Timms K, Tiwari S, Tixeira R, Tkach M, Toh WS, Tomasini R, Torrecilhas AC, Tosar JP, Toxavidis V, Urbanelli L, Vader P, van Balkom BW, van der Grein SG, Van Deun J, van Herwijnen MJ, Van Keuren-Jensen K, van Niel G, van Royen

ME, van Wijnen AJ, Vasconcelos MH, Vechetti IJ, Jr., Veit TD, Vella LJ, Velot É, Verweij FJ, Vestad B, Viñas JL, Visnovitz T, Vukman KV, Wahlgren J, Watson DC, Wauben MH, Weaver A, Webber JP, Weber V, Wehman AM, Weiss DJ, Welsh JA, Wendt S, Wheelock AM, Wiener Z, Witte L, Wolfram J, Xagorari A, Xander P, Xu J, Yan X, Yáñez-Mó M, Yin H, Yuana Y, Zappulli V, Zarubova J, Žėkas V, Zhang JY, Zhao Z, Zheng L, Zheutlin AR, Zickler AM, Zimmermann P, Zivkovic AM, Zocco D, Zuba-Surma EK. Minimal information for studies of extracellular vesicles 2018 (MISEV2018): a position statement of the International Society for Extracellular Vesicles and update of the MISEV2014 guidelines. J Extracell Vesicles 2018; 7: 1535750

Timmerman LA, Grego-Bessa J, Raya A, Bertrán E, Pérez-Pomares JM, Díez J, Aranda S, Palomo S, McCormick F, Izpisúa-Belmonte JC, de la Pompa JL. Notch promotes epithelial-mesenchymal transition during cardiac development and oncogenic transformation. Genes Dev 2004; 18: 99-115

Uchida S, Dimmeler S. Long noncoding RNAs in cardiovascular diseases. Circ Res 2015; 116: 737-750

Wang J, Chen L, Li H, Yang J, Gong Z, Wang B, Zhao X. Clopidogrel reduces apoptosis and promotes proliferation of human vascular endothelial cells induced by palmitic acid via suppression of the long non-coding RNA HIF1A-AS1 in vitro. Mol Cell Biochem 2015; 404: 203-210

Wang Y, Liang J, Xu J, Wang X, Zhang X, Wang W, Chen L, Yuan T. Circulating exosomes and exosomal lncRNA HIF1A-AS1 in atherosclerosis. Int J Clin Exp Pathol 2017; 10: 8383-8388

Widmer RJ, Lerman A. Endothelial dysfunction and cardiovascular disease. Glob Cardiol Sci Pract 2014; 2014: 291-308

Willems IE, Havenith MG, Smits JF, Daemen MJ. Structural alterations in heart valves during left ventricular pressure overload in the rat. Lab Invest 1994; 71: 127-133

Wirrig EE, Yutzey KE. Conserved transcriptional regulatory mechanisms in aortic valve development and disease. Arterioscler Thromb Vasc Biol 2014; 34: 737-741

Xiong G, Jiang X, Song T. The overexpression of lncRNA H19 as a diagnostic marker for coronary artery disease. Rev Assoc Med Bras (1992) 2019; 65: 110-117

Xu J, Zhang Y, Chu L, Chen W, Du Y, Gu J. Long non-coding RNA HIF1A-AS1 is upregulated in intracranial aneurysms and participates in the regulation of proliferation of vascular smooth muscle cells by upregulating TGF-β1. Exp Ther Med 2019; 17: 1797-1801

Yu B, Wang S. Angio-LncRs: LncRNAs that regulate angiogenesis and vascular disease. Theranostics 2018; 8: 3654-3675

Zhang C, Xu X, Potter BJ, Wang W, Kuo L, Michael L, Bagby GJ, Chilian WM. TNF-alpha contributes to endothelial dysfunction in ischemia/reperfusion injury. Arterioscler Thromb Vasc Biol 2006; 26: 475-480

Zhang K, Qi Y, Wang M, Chen Q. Long non-coding RNA HIF1A-AS2 modulates the proliferation, migration, and phenotypic switch of aortic smooth muscle cells in aortic dissection via sponging microRNA-33b. Bioengineered 2022; 13: 6383-6395

Zhang X, Li H, Guo X, Hu J, Li B. Long Noncoding RNA Hypoxia-Inducible Factor-1 Alpha-Antisense RNA 1 Regulates Vascular Smooth Muscle Cells to Promote the Development of Thoracic Aortic Aneurysm by Modulating Apoptotic Protease-Activating Factor 1 and Targeting let-7g. J Surg Res 2020; 255: 602-611

Zhao G, Su Z, Song D, Mao Y, Mao X. The long noncoding RNA MALAT1 regulates the lipopolysaccharide-induced inflammatory response through its interaction with NF-κB. FEBS Lett 2016; 590: 2884-2895

Zietzer A, Hosen MR, Wang H, Goody PR, Sylvester M, Latz E, Nickenig G, Werner NJansen F. The RNA-binding protein hnRNPU regulates the sorting of microRNA-30c-5p into large extracellular vesicles. J Extracell Vesicles 2020; 9: 1786967

9. Acknowledgments

I would like to thank all those who helped me during the study in Bonn and the writing of this thesis.

First of all, I would like to express my sincere gratitude to my supervisor PD. Dr. med. Felix Jansen. I gratefully acknowledge the help of his supervision and his valuable suggestions during the process of my research.

Second, I give my great appreciation to the supervisor and mentor for this project, Dr. rer. nat. Mohammed Rabiul Hosen. He has offered me valuable ideas, suggestions and criticisms with his profound knowledge and rich research experience. He is a very supportive, cheerful, and energetic researcher and gave me lots of helpful information. I am very much obliged to his efforts of helping me complete this dissertation.

Third, I am also grateful to all the colleagues in the lab who have helped me with my research. I must express my thanks to Dr. med. Philip Goody, Ms Katharina Maus, Ms. Sarah Arahouan, Ms. Anna Flender, and Mr. Yuan Zhou for their assistance.

Last but not least, I would like to express my special thanks to my beloved parents, I will always be grateful for their love.